Supporting information

Labeling of Proteins by BODIPY-Quinone Methides utilizing Anti-Kasha Photochemistry

Katarina Zlatić,[a] Ivana Antol,*[a] Lidija Uzelac,[b] Ana-Matea Mikecin Dražić,[b,c] Marijeta Kralj,*[b] Cornelia Bohne,[d,e] Nikola Basarić[a]*

[a] Department of Organic Chemistry and Biochemistry, Ruđer Bošković Institute, Bijenička cesta 54, 10 000 Zagreb, Croatia. Fax: + 385 1 4680 195, E-mail: IA iantol@irb.hr; NB nbasaric@irb.hr

[b] Department of Molecular Medicine, Ruđer Bošković Institute, Bijenička cesta 54, 10 000 Zagreb, Croatia. E-mail: marijeta.kralj@irb.hr

[c] Current address: Division of Experimental Hematology, German Cancer Research Center (DKFZ) HI-STEM gGmbH, Im Neuenheimer Feld 280, 69120 Heidelberg, Germany

[d] Department of Chemistry, University of Victoria, Box 1700 STN CSC, Victoria BC.

[e] Centre for Advanced Materials and Related Technologies (CAMTEC), University of Victoria, Box 1700 STN CSC, Victoria BC, V8W 2Y2, Canada

Content:

1. Synthetic procedures

General

^{1}H and ^{13}C NMR spectra were recorded on a Bruker AV- 300, or 600 MHz. The NMR spectra were taken in $CDCl_3$, CD_3OD or DMSO-d_6 at rt using TMS as a reference. HRMS were obtained on an Applied Biosystems 4800 Plus MALDI TOF/TOF instrument (AB, Foster City, CA). Analytical thin layer chromatography was performed on Polygram® SILG/UV_{254} (Machery-Nagel) plates. Chemicals for the synthesis were purchased from the usual suppliers (Sigma-Aldrich, TCI, Alfa Aesar, etc), whereas solvents for the synthesis and chromatographic separations were purified by distillation, or used as received (p.a. grade). Silica gel (0.05–0.2 mm) was used for chromatographic purifications. The analysis of photochemical reaction mixtures was performed on a Shimadzu HPLC equipped with a diode-array detector and a Phenomenex Luna 3u C18(2) column. Mobile phase was CH_3OH-H_2O (+0.1% TFA) 1:1 10 min, CH_3OH (50%→100%, 10→20 min, and CH_3OH (100%) 40 min, the flow rate was 0.8 mL/min.

Preparation of 5-(4-hydroxyphenyl)dipyrromethane (5)[1]

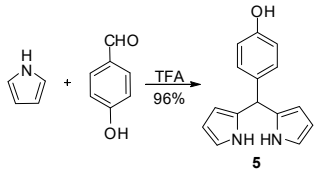

5

Scheme S1.

4-Hydroxybenzaldehyde (1.0 g, 8.4 mmol) was dissolved in pyrrole (14 mL, 215 mmol), and the solution was degassed. TFA (100 µL) was added and the reaction mixture was stirred for 10 min at rt. The reaction was quenched by addition of aqueous NaOH solution (1 M) following by extraction with ethyl acetate. The organic extracts were washed with H_2O and dried over anhydrous $MgSO_4$. The solvent and excess pyrrole were removed by vacuum distillation. The residue was dissolved in CH_2Cl_2 and chromatographed on a column filled with silica using CH_2Cl_2/EtOAc as eluent. The title compound was obtained (1.93 g, 96%).

^{1}H NMR ($CDCl_3$, 300 MHz) δ/ppm: 7.90 (br s, 2H), 7.08 (d, 2H, J = 8.6 Hz), 6.77 (d, 2H, J = 8.6 Hz), 6.89 (dd, 2H, J = 2.7 Hz, J = 2.3 Hz), 6.15 (dd, 2H, J = 2.7 5 Hz, J = 3.1 Hz), 5.91 (br s, 2H), 5.42 (s, 1H), 4.67 (br s, 1H).

Preparation of 5-(4-hydroxyphenyl)dipyrrin (6)[1]

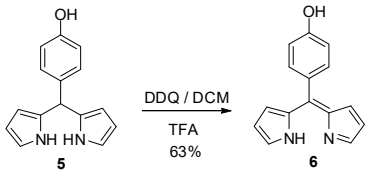

Scheme S2.

Compound **5** (700 mg, 3.0 mmol) was dissolved in dried CH_2Cl_2 (30 mL). The solution was purged with argon and a drop of TFA was added. The reaction mixture was stirred for 4 h under argon followed by the addition of DDQ (680 mg, 3.0 mmol) in CH_2Cl_2 (5 mL). The stirring was continued for 2 h, the solvent was removed on a rotary evaporator and the residue was chromatographed on a column of silica gel using CH_2Cl_2/EtOAc (15 %) as eluent. The title compound **4** was obtained (440 mg, 63 %).

Brown crystals; ^{1}H NMR ($CDCl_3$, 300 MHz) δ/ppm: 7.64 (br s, 2H), 7.39 (d, 2H, J = 8.4 Hz), 6.85 (d, 2H, J = 8.4 Hz), 6.71 (d, 2H, J = 4.7 Hz), 6.46 (dd, 2H, J = 4.7, J = 1.5 Hz), 5.00 (br s, 1H, OH), NH not observed; ^{1}H NMR (DMSO-d_6, 300 MHz) δ/ppm: 7.77 (br s, 2H), 7.34 (d, 2H, J = 8.8 Hz), 6.89 (d, 2H, J = 8.8 Hz), 6.70 (br s, 2H), 6.51 (br s, 2H), 3.50 (OH associated with DMSO and H_2O), NH not observed; ^{13}C NMR (DMSO-d_6, 75 MHz) δ/ppm: 144.9 (s), 143.0 (s), 138.7 (d), 134.7 (d), 129.4 (d), 127.7 (s), 118.0 (d), 116.7 (d), one singlet was not observed.

Preparation of 4,4-Difluoro-8-(4-hydroxyphenyl)-4-bora-3a,4a-diaza-s-indacene (7)[1]

Scheme S3.

A toluene solution of one equivalent of dipyrrin (**6**, 440 mg, 1.86 mmol) was purged with argon. To the solution, triethylamine (2.6 mL, 18.6 mmol) was added, and the solution was heated at 70 °C for 0.5 h. Then, BF_3 etherate (3.2 g, 7.1 mL, 22.3 mmol) was added and the reaction mixture was heated at the temperature of reflux for 2 h. To the cooled reaction mixture, an aqueous solution of NaOH (1 M, 25 mL) was added. The layers were separated and the aqueous layer was brought to pH 5-6 by addition of HCl. The aqueous layer was extracted with CH_2Cl_2 and EtOAc, dried over anhydrous $MgSO_4$, and the solvent was removed by distillation. The

residue was chromatographed on silica using CH_2Cl_2/EtOAc as eluent to afford the title product 340 mg (64 %).

Orange crystals; ^{1}H NMR ($CDCl_3$, 300 MHz) δ/ppm: 7.93 (br s, 2H), 7.47 (d, 2H, J = 8.8 Hz), 6.99 (br s, 2H), 6.97 (d, 2H, J = 8.8 Hz), 6.56 (br s, 2H), 6.15 (br s, 1H, OH); ^{13}**C** NMR ($CDCl_3$, 75 MHz) δ/ppm: 159.1 (s), 147.9 (s), 143.8 (d), 135.2 (s), 133.0 (d), 131.8 (d), 126.6 (s), 118.8 (d), 116.0 (d).

Synthesis of 4,4-difluoro-8-[3-(*N*,*N*-dimethylaminomethyl)-4- hydroxyphenyl]-4-bora-3a,4a-diaza-s-indacene (1)

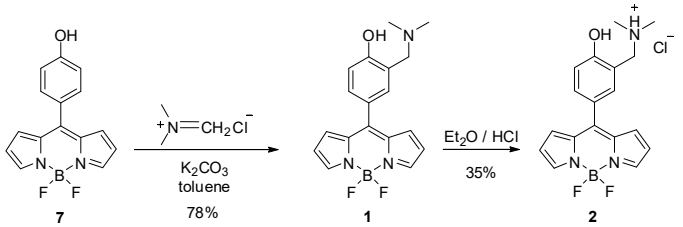

Scheme S4.

BODIPY **7** (500 mg, 1.76 mmol), anhydrous K_2CO_3 (365 mg, 2.64 mmol) and the Eschenmoser's salt (*N*,*N*-dimethylmethyleneiminium chloride, 246 mg, 2.64 mmol) were added to anhydrous toluene (50 mL). The reaction mixture was refluxed over night. The next day, the toluene was poured off, the dark tarry residue washed with EtOAc (3×75 mL) and filtered through a sinter funnel. The organic solutions were combined and evaporated yielding crude product which was purified on a column of Al_2O_3 (activity IV) using CH_2Cl_2-EtOAc (0→100%) as eluent. The crude title product (470 mg, 78%) in the form of orange crystals was obtained, which was transformed to the corresponding HCl salt without further purification.

Synthesis of 4,4-difluoro-8-[3-(*N*,*N*-dimethylammoniummethyl)-4-hydroxyphenyl]-4-bora-3a,4a-diaza-s-indacene hydrochloride (2)

Amine **1** obtained in the above reaction (470 mg, 1.37 mmol) was dissolved in anhydrous diethyl ether (Et_2O, 10 mL) to which Et_2O saturated with HCl was added dropwise until further additions did not result in precipitate formation. The precipitate was filtered off on a Hirsch sinter funnel (G4), washed with Et_2O and dried in a desiccator over KOH.

Orange crystals (230 mg, 35% in two steps) mp 174-175 °C; ^{1}H NMR (600 MHz, DMSO-d_6) δ/ppm: 11.28 (br s, 1H), 9.87 (br s, 1H), 8.09 (br s, 2H), 7.80 (d, 1H, J = 2.2 Hz), 7.66 (dd, 1H, J = 2.2 Hz, J = 8.5 Hz), 7.23 (d, 1H, J = 8.5Hz), 7.18 (d, 2H, J = 4.0 Hz), 6.70 (dd, 2H, J = 1.8 Hz, J = 4.0 Hz), 4.32 (s, 2H), 2.79 (s, 6H); ^{1}H NMR (CD_3OD, 300 MHz) δ/ppm: 7.95 (br s,

2H), 7.31 (br s, 2H), 7.18 (d, 1H, J = 8.4 Hz), 7.08 (d, 2H, J = 4.1 Hz), 6.64 (dd, 2H, J = 1.4 Hz, J = 4.2 Hz), 4.43 (s, 2H), 2.92 (s, 6H); ^{13}C NMR (CD_3OD, 75 MHz) δ/ppm: 159.3 (s), 146.4 (s), 143.7 (d), 135.0 (d), 134.5 (s), 134.4 (d), 131.1 (d), 125.4 (s), 118.3 (d), 117.1 (s), 115.4 (d), 56.4 (t), 42.1 (q); HRMS (MALDI-TOF/TOF) calculated for $C_{18}H_{19}BF_2N_3O$ 342.1589; found 342.1581.

Synthesis of 2,4,6,8-tetramethyl-5-(4-hydroxyphenyl)dipyrromethane (6)[2]

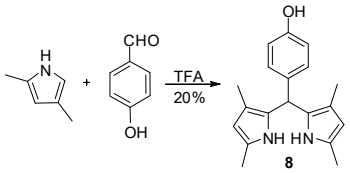

Scheme S5.

4-Hydroxybenzaldehyde (1.22 g, 10 mmol) was dissolved in dry dichloromethane (40 mL). To the solution 2,4-dimethylpyrrole (2.30 g, 20.72 mmol) was added. The solution was purged with N_2, and TFA (100 μL) was added. The reaction mixture was stirred at rt for 2 h. The reaction was quenched by addition of aqueous sodium hydroxide solution (1 M, 30 mL) following by extraction with EtOAc (3×50 mL). The organic extracts were washed with water (30 mL) and dried over anhydrous $MgSO_4$. The aqueous layer was neutralized, and extraction with EtOAc (3×50 mL) was conducted. The extracts were dried over anhydrous $MgSO_4$ and the solvent was removed on a rotary evaporator. The residue was chromatographed on a column of silica gel using CH_2Cl_2 and EtOAc as eluent to afford the pure title product (600 mg, 20%). ^{1}H NMR ($CDCl_3$, 300 MHz) δ/ppm: 7.20 (br s, 2H), 7.00 (d, 2H, J = 8.4 Hz), 6.76 (d, 2H, J = 8.4 Hz), 5.69 (d, 2H, J = 2.1 Hz), 5.36 (s, 1H), 2.14 (s, 6H), 1.81 (s, 6H).

Synthesis of 4,4-Difluoro-8-(4-hydroxyphenyl)-1,3,5,7-tetramethyl-4-bora-3a,4a-diaza-s-indacene (9)[3]

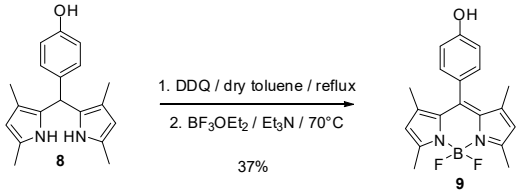

Scheme S6.

Compound **8** (800 mg, 2.72 mmol) and DDQ (680 mg, 3.0 mmol) were suspended in dry toluene (50 mL). The suspension was heated at reflux 1 h. To the cooled reaction mixture triethylamine was added (4 mL, 28.7 mmol), followed by BF_3 etherate (6 mL, 20.5 mmol). The reaction

mixture was heated at 70 °C over night. To the cooled reaction mixture, an aqueous solution of NaOH (1M, 30 mL) was added and the layers were separated. The aqueous layer was neutralized with 4 M HCl, and extraction with EtOAc (3×50 mL) was carried out. The combined organic layers were dried over anhydrous $MgSO_4$, filtered, and the solvent was removed on a rotary evaporator. The residue was chromatographed on a column of silica gel using CH_2Cl_2/EtOAc as eluent to afford the pure title product (350 mg, 37%).

^{1}H NMR ($CDCl_3$, 300 MHz) δ/ppm: 7.12 (d, 2H, J = 8.4 Hz), 6.94 (d, 2H, J = 8.4 Hz), 5.97 (br s, 2H), 5.18 (br s, 1H), 2.54 (s, 6H), 2.14 (s, 6H).

Synthesis of 4,4-difluoro-1,3,5,7-tetramethyl-8-[3-(N,N-dimethylaminomethyl)-4-hydroxyphenyl]-4-bora-3a,4a-diaza-s-indacene (3)

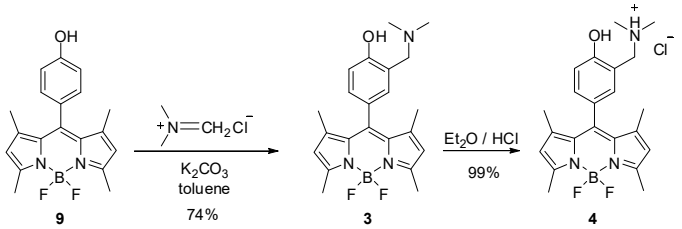

Scheme S7.

Compound **7** (280 mg, 0.85 mmol), anhydrous potassium carbonate (177 mg, 1.28 mmol) and Eschenmoser's salt (*N*,*N*-dimethylmethyleneiminium chloride, 120 mg, 1.28 mmol) were added to anhydrous toluene (50 mL). The reaction mixture was refluxed over night. The next day the toluene was poured off, the dark tarry residue washed with EtOAc (3×75 mL) and filtered through a sinter funnel. The organic solutions were combined and evaporated yielding crude product which was purified on a column of Al_2O_3 (activity IV) using CH_2Cl_2-EtOAc (0→100%) as eluent. The title product (250 mg, 74%) was obtained in the form of orange crystals.

mp 165-166 °C; ^{1}H NMR ($CDCl_3$, 300 MHz) δ/ppm: 7.05 (dd, 1H, J = 2.0 Hz, J = 8.2 Hz), 6.95 (d, 1H, J = 8.2 Hz), 6.86 (d, 1H, J = 2.0 Hz), 5.96 (br s, 2H), 3.69 (s, 2H), 2.54 (s, 6H), 2.36 (s, 6H), 1.45 (s, 6H).

Synthesis of 4,4-difluoro-1,3,5,7-tetramethyl-8-[3-(*N*,*N*-dimethylammoniummethyl)-4-hydroxyphenyl]-4-bora-3a,4a-diaza-s-indacene hydrochloride (4)

Amine **3** obtained in the above reaction (200 mg, 0.50 mmol) was dissolved in anhydrous diethyl ether (Et_2O, 10 mL), to which Et_2O saturated with HCl was added dropwise until further additions did not result in precipitate formation. The precipitate was filtered off on a Hirsch

sinter funnel (G4), washed with Et_2O and dried in a desiccator over KOH. The title product (215 mg, 99%) was obtained in the form of orange crystals.

mp 186-187 °C; ^{1}H NMR (300 MHz, DMSO-d_6) δ/ppm: 10. 81 (br s, 1H), 9.65 (br s, 1H), 7.38 (d, 1H, J = 2.1 Hz), 7.28 (dd, 1H, J = 2.1 Hz, J = 8.3 Hz), 7.15 (d, 1H, J = 8.3 Hz), 6.19 (br s, 2H), 4.27 (s, 2H), 2.73 (s, 6H), 2.45 (s, 6H), 1.45 (s, 6H); ^{1}H NMR (CD_3OD, 300 MHz) δ/ppm: 7.34-7.30 (m, 2H), 7.16 (d, 1H, J = 8.3 Hz), 6.10 (br s, 2H), 4.40 (s, 2H), 2.90 (s, 6H), 2.50 (s, 6H), 1.52 (s, 6H); ^{13}C NMR (CD_3OD, 75 MHz) δ/ppm: 157.4 (s), 155.4 (s), 142.9 (s), 141.1 (s), 131.9 (d), 131.7 (d), 126.4 (s), 120.9 (d), 117.7 (s), 116.0 (d), 56.6 (t), 42.0 (q), 13.6 (q), 13.2 (q); calculated for $C_{22}H_{27}BF_2N_3O$ 398.2215; found 398.2210.

Photochemical experiments

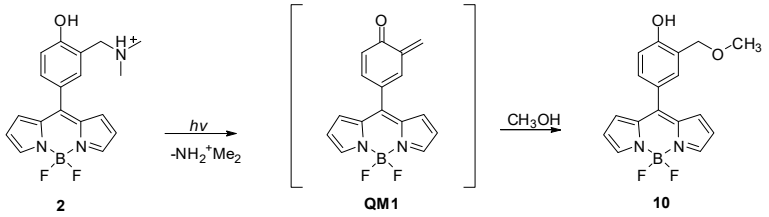

Scheme S8. Photomethanolysis of **2**

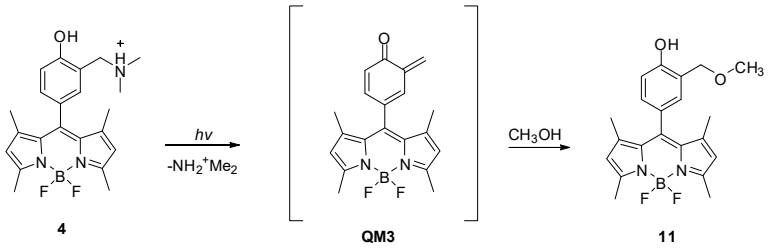

Scheme S9. Photomethanolysis of **4**

BODIPY-QM precursors **2** or **4** (3 mg) were dissolved in CH_3OH, or CH_3OH-H_2O (5:1) buffered with sodium phosphate buffer (c = 0.05 M) at pH 7.0 or 9.0. The solutions were purged with N_2 for 15 min, sealed and irradiated in u Luzchem reactor equipped with 8 lamps (cool white, 350 nm, 300 nm, or 254 nm, each lamp 8W). The composition of the irradiated mixture was analyzed by HPLC (Table S1). After the irradiations, an analysis by HPLC-MS was performed. The solvent was removed on a rotary evaporator and the residue was analyzed by ^{1}H NMR. To isolate photoproducts, combined residues after different irradiation experiments were chromatographed on a column of silica gel using CH_2Cl_2 as eluent.

4,4-difluoro-8-(3-methoxymethyl-4-hydroxyphenyl)-4-bora-3a,4a-diaza-s-indacene (10)

mp 81 - 82°C; ^{1}H NMR (CD_3OD, 300 MHz) / ppm: 7.81 (s, 2H), 7.49 (d, 1H, J = 2.1 Hz), 7.38 (dd, 1H, J = 2.2 Hz, 8.3 Hz), 6.97 (d, 1H, J = 24.1 Hz), 6.53 (d, 2H, J = 2.7 Hz), 4.49 (s, 2H), 3.37 (s, 3H); ^{13}C NMR (CD_3OD, 75 MHz, APT) / ppm: 142.8 (d), 131.9 (d), 131.7 (d), 131.1 (d), 117.9 (d), 114.8 (d), 68.9 (t), 57.4 (q), signals of the quaternary C-atoms were not observed; HPLC-MS (ESI) ***m/z:*** 327.1 (M-); HRMS (MALDI-TOF/TOF) calculated for $C_{17}H_{15}BF_2N_2O_2$ 328.1195; found 328.1205.

4,4-difluoro-1,3,5,7-tetramethyl-8-(3-methoxymethyl-4-hydroxyphenyl)-4-bora-3a,4a-diaza-s-indacene (11)

mp 110 - 111°C; ^{1}H NMR (CD_3OD, 300 MHz) / ppm: 7.16 (d, 1H, J = 2.1 Hz), 7.16 (dd, 1H, J = 2.3 Hz, 8.0 Hz), 4. 29 (d, 1H, J = 8.3 Hz), 6.05 (s, 2H), 4.55 (s, 2H), 3.39 (s, 3H), 2.84 (s, 6H), 1.49 (s, 6H); ^{13}C NMR (CD_3OD, 75 MHz, APT) / ppm: 156.2 (s), 154.9 (s), 143.2 (s), 128.8 (d), 128.2 (d), 125.6 (s), 125.3 (s), 120.6 (d), 115,4 (d), 69.0 (t), 57.0 (q), 13.4 (q), 13.1 (q); HPLC-MS (ESI) ***m/z:*** 383.1 (M-); HRMS (MALDI-TOF/TOF) calculated for $C_{21}H_{23}BF_2N_2O_2$ 384.1821; found 384.1824.

Table S1. Yields (%) for photoproducts **10** and **11** upon irradiation of **2** and **4**, respectively at different wavelengths (irradiation 16 h, unless stated otherwise).

Compound/conditions	254 nm	300 nm	350 nm	vis (cool white)
2 / CH_3OH	decomp.	2	N. R.	N. R.
2 / CH_3OH-H_2O (1:1), pH 7	68	42	2	< 1
2 / CH_3OH-H_2O (1:1), pH 9	decomp.	52	8	< 1
4 / CH_3OH	30 (9h)	12 (12 h)	1	N. R.
4 / CH_3OH-H_2O (1:1), pH 7	100 (2h)	100 (6h)	21	2
4 / CH_3OH-H_2O (1:1), pH 9	94 (4h)	100 (6h)	19	2

Quantum yield for photomethanolysis of 4 upon excitation at 254 nm

The quantum yield for the photomethanolysis reaction was determined by using KI/KIO_3 (Φ_{254} = 0.74)[4] as an actinometer. A solution of compound **4** in CH_3OH-H_2O (5:1), buffered with sodium phosphate buffer (c = 0.05 M, pH 7.0) was prepared with a concentration corresponding

to an absorbance $A \approx 0.7$ at 254 nm. The solution was purged with an Ar stream (15 min) and then sealed with a cap. The solutions of compound and the actinometer were irradiated in quartz cuvettes, at the same time with one lamp (254 nm, 8W). For compound **4** formation of products **11** was measured by HPLC and the obtained values were used for the calculation of quantum yields (Eq. S1-S5). Measurements were carried out three times in three independent experiments, and the average value is reported.

The **number of absorbed photons for the KIO_3/KI** was calculated from:

$$n(\text{absorbed photons}) = \frac{\Delta A_{352} \times V_{irr}}{\varepsilon_{352} \times \ell \times \Phi_{lit.}} \qquad \text{(S1)}$$

where:

ΔA_{352}	absorbance difference at 352 nm for the irradiated and non-irradiated sample
V_{irr}	volume of the solution which was irradiated
ε_{352}	molar absorption coefficient for I_3^- in solution which contains iodides and iodates, 27600 M^{-1} cm^{-1}
l	length of the optical path (1 cm in all experiments)
$\Phi_{lit.}$	quantum yield ($\Phi_{254} \approx 0.74$), the precise value was calculated from S2 and S3 (depending on the iodine concentration and temperature)

$$c(I^-) = A_{300} / 1.061 \quad [M] \qquad \text{(S2)}$$

$$\Phi_{lit} = 0.75 \times [1 + 0.02(T - 20.7)] \times [1+0.23(c(I^-) - 0.577)] \qquad \text{(S3)}$$

For the absorbances in the range 0.4-0.8 the number of absorbed photons was calculated according to:

$$n(\text{absorbed photons}) = n(\text{total photons}) \times (1\text{-}T) \qquad \text{(S4)}$$

The quantum yield for the photohydrolysis was calculated according to:

$$\Phi = \frac{A_{254} \cdot V_{\text{irr}} \cdot x(\text{photoproduct})_{\text{HPLC}}}{\varepsilon_{254} \cdot \ell \cdot n(\text{total photons}) \cdot (1 - T_{254})} \qquad \text{(S5)}$$

where:

$x(\text{photoproduct})_{\text{HPLC}}$ conversion of reactant to photoproduct determined by HPLC

T_{254} transmittance of light at 254 nm

2. UV-vis and fluorescence spectroscopy

UV-Vis spectra were recorded on a Varian Cary 100 Bio spectrophotometer at 20°C. Fluorescence measurements were performed on a PTI QM40 fluorometer at 20°C. All slits (excitation and emission) were set to the bandpass of 2 nm. The spectra were corrected for the fluctuations in lamp intensity and transmission of optics. The samples were excited at 450, 460 or 470 nm, and the emission was collected in the range of 475-700 nm. For the excitation spectra, emission was detected at 520, 530 and 540 nm, and the excitation was scanned in the range 300-520 nm. Fluorescence quantum yields were determined by the use of rhodamine 6G in CH_3OH as a reference (Φ_F = 0.86).[5] Prior to the measurements, the solutions were purged with a stream of N_2 for 15 min. Three quantum yields were measured by exciting at three wavelentgths (Eq. 6) and the average value is reported (Table S2).

The following equation was used for the determination of fluorescence quantum yields:

$$\Phi = \Phi_R \frac{I}{I_R} \frac{A_R}{A} \left(\frac{n_D}{n_D^R}\right)^2 \qquad \text{(S6)}$$

wherein

Φ - quantum yield of fluorescence

Φ_R - quantum yield of fluorescence of reference compound, Fluorescence quantum yields were measured using rhodamine 6G in CH_3OH as a reference (Φ_f = 0.86)5

I - intensity of fluorescence (integral of the corrected emission spectrum)

I_R - intensity of fluorescence (integral of the corrected emission spectrum) for the reference compound

A - absorbance of the solution at the excitation wavelength

A_R - absorbance of the solution of the reference compound at the excitation wavelength

n_D - refractive index of the solvent

n_D^R - refractive index of the solvent used to dissolve the reference compound (CH_3OH)

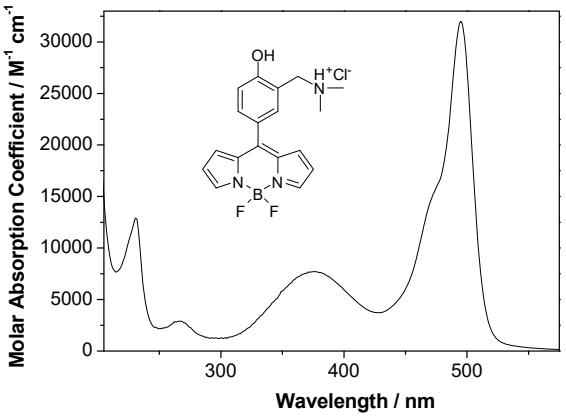

Figure S1. Absorption spectrum of **2** in CH_3CN.

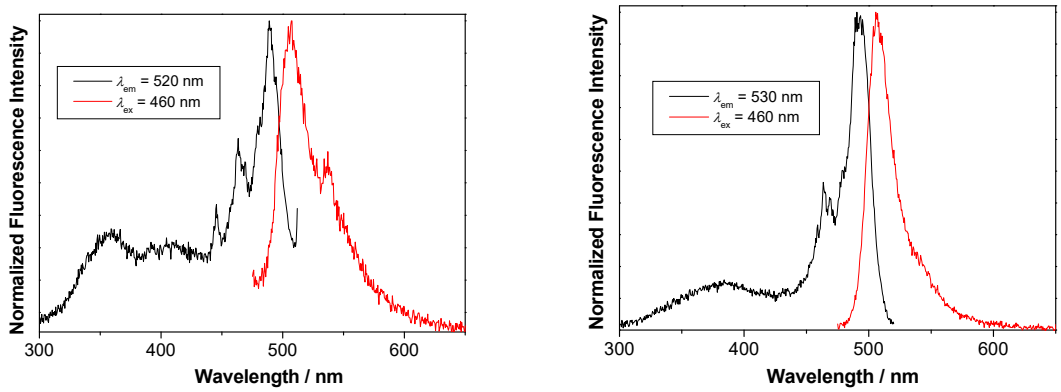

Figure S2. Normalized excitation and emission of **2** in CH_3CN (left) and CH_3CN-H_2O (1:9) (right).

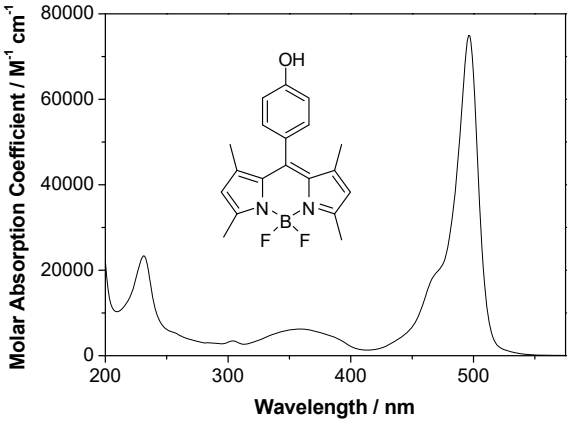

Figure S3. Absorption spectrum of **9** in CH_3CN.

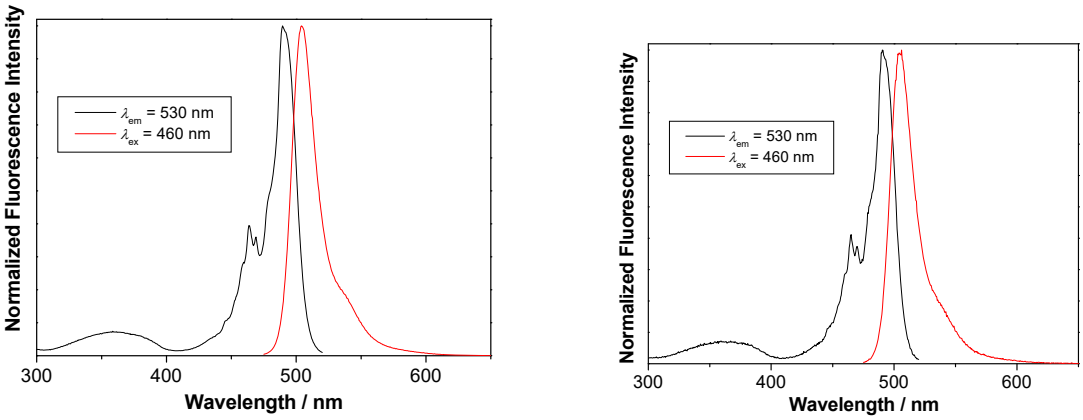

Figure S4. Normalized excitation and emission of **9** in CH_3CN (left) and CH_3CN-H_2O (1:9) (right).

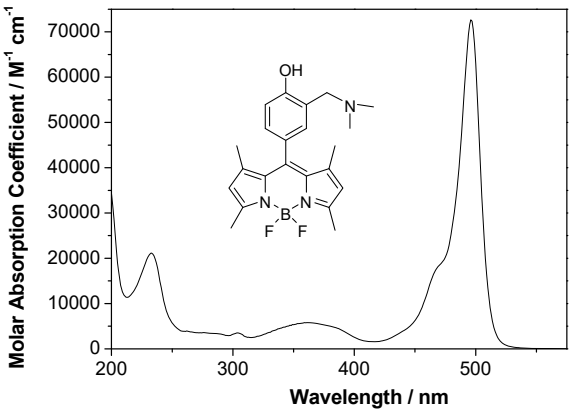

Figure S5. Absorption spectrum of **3** in CH_3CN.

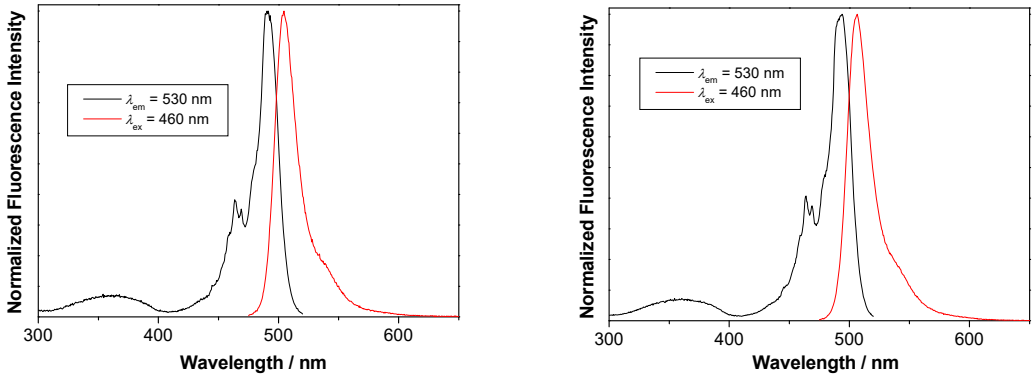

Figure S6. Normalized excitation and emission of **3** in CH_3CN (left) and CH_3CN-H_2O (1:9) (right).

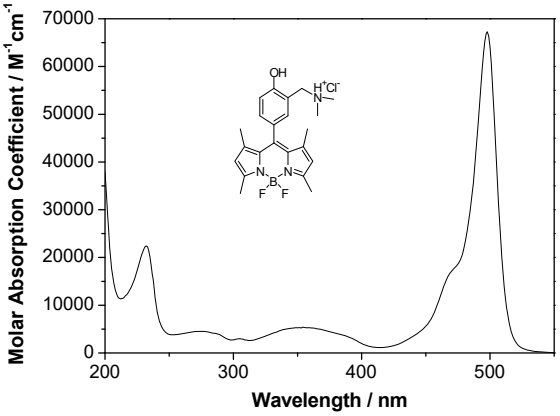

Figure S7. Absorption spectrum of **4** in CH_3CN.

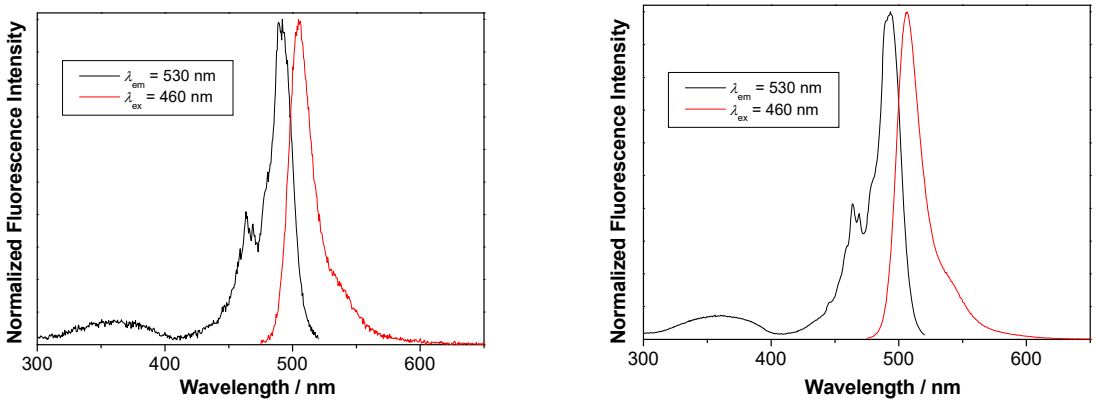

Figure S8. Normalized excitation and emission of **4** in CH_3CN (left) and CH_3CN-H_2O (1:9) (right).

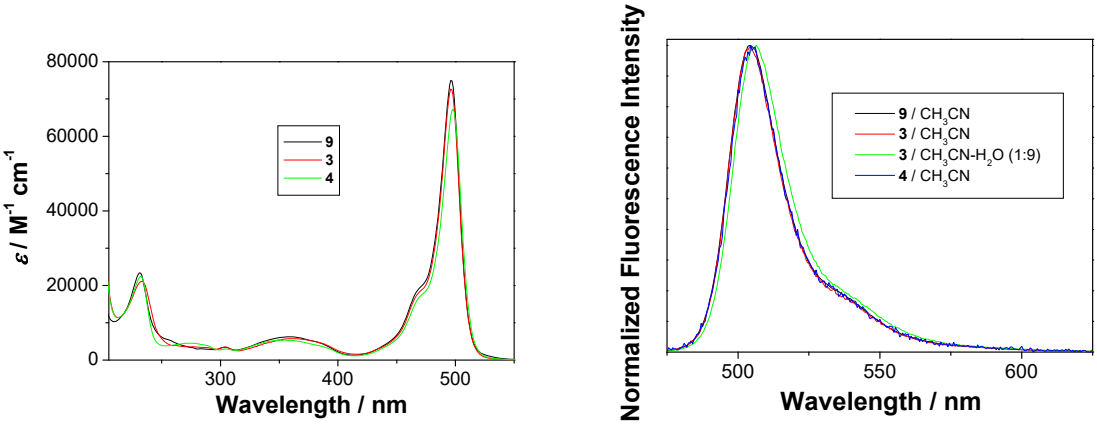

Figure S9. Absorption spectra in CH_3CN (left) and normalized emission spectra in CH_3CN or CH_3CN-H_2O (1:9) for different BODIPY derivatives.

Fluorescence decays, collected over 1023 time channels, were obtained on an Edinburgh Instruments OB920 single photon counter using a pulsed laser diode for excitation at 375 nm. The instrument response functions, using LUDOX as the scatterer, were recorded at the same wavelengths as the excitation wavelength and had a half width of ≈ 0.2 ns. The time increment per channel was 0.020 ns. Emission decays were recorded until they reached 2×10^3 counts in the peak channel at 510, 520, and 530 nm. Global analysis of decays was performed by fitting to sum of exponentials using global Gaussian-weighted non-linear least-squares fitting based on the Marquardt-Levenberg minimization algorithm implemented in the Fast software package from Edinburgh Instruments. The fitting parameters (decay times and pre-exponential factors, Eq. S7) were determined by minimizing the reduced chi-square χ^2 and graphical methods were used to judge the quality of the fit that included plots of the weighted residuals vs. channel number. Decay times were kept linked for decays collected over different wavelengths.

Fluorescence decays, were fit as sums of exponentials using Gaussian-weighted non-linear least-squares fitting based on the Marquardt-Levenberg minimization algorithm implemented in the Fast software.

Fluorescence decays were fit to a sum of exponentials using the following expression:

$$F\,(t) = \alpha_1 \exp\left(-\frac{t}{\tau_1}\right) + \alpha_2 \exp\left(-\frac{t}{\tau_2}\right) + \alpha_3 \exp\left(-\frac{t}{\tau_3}\right) + \ \ldots \qquad \text{(S7)}$$

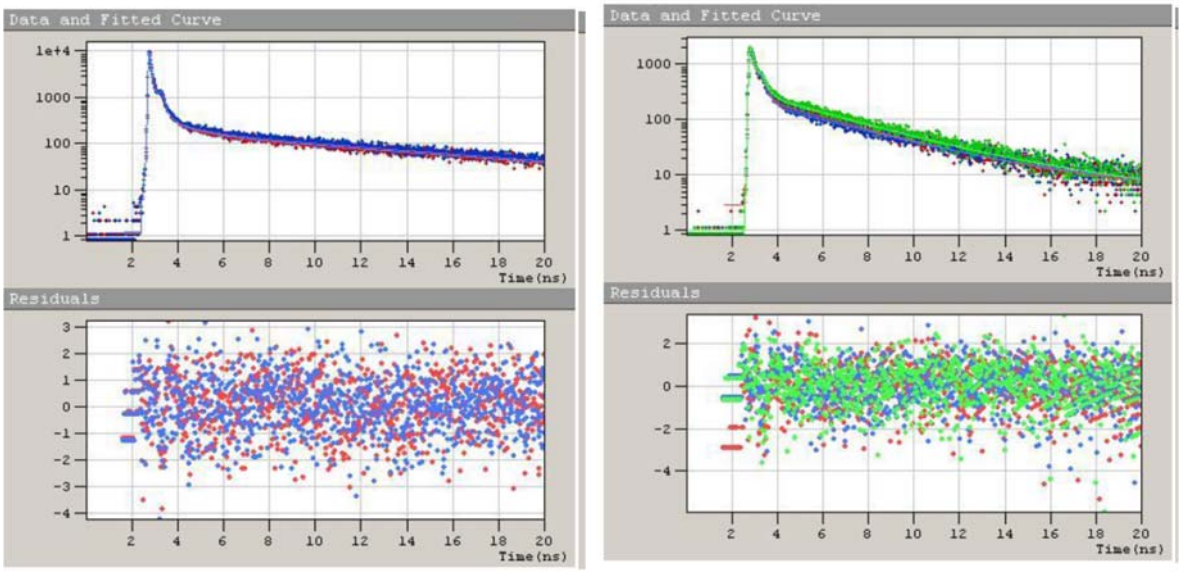

Figure S10. Global fitting of decays obtained by SPC for **2** in CH_3CN (left) and CH_3CN-H_2O (right), λ_{ex} = 375 nm, λ_{em} 510 and 520 nm (left) and 510, 520 and 530 nm (right). The bottom panels of the figures correspond to residuals between the fitted and experimental values.

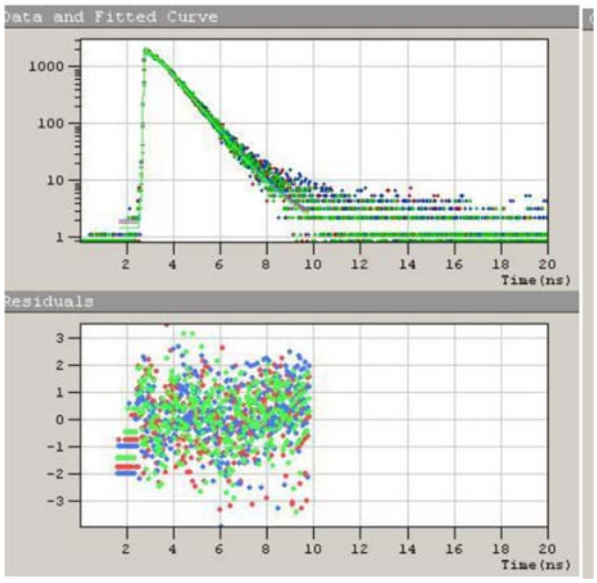

Figure S11. Global fitting of decays obtained by SPC for **9** in CH_3CN-H_2O, λ_{ex} = 375 nm, λ_{em} = 510, 520 and 530 nm. The bottom panel of the figure corresponds to residuals between the fitted and experimental values.

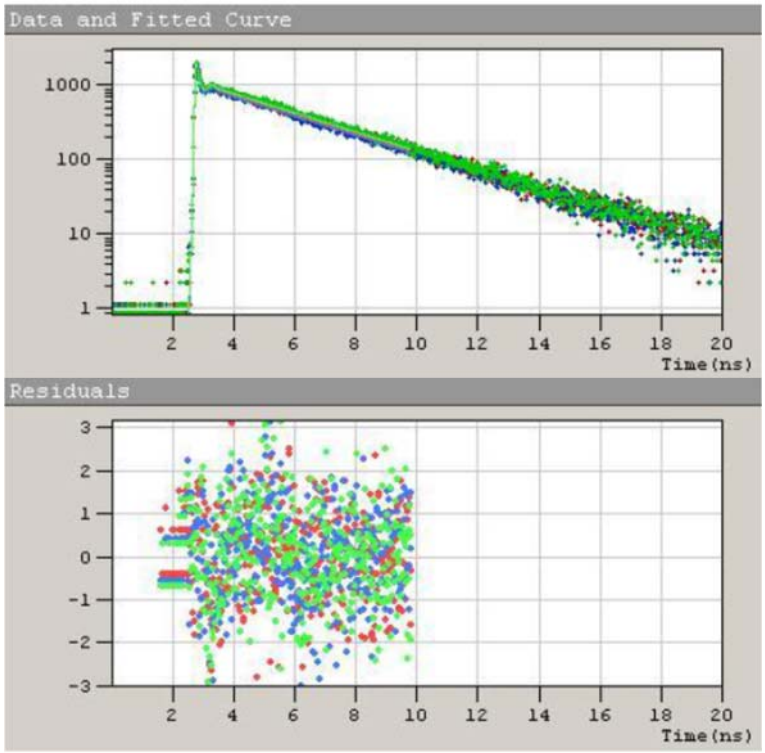

Figure S12. Global fitting of decays obtained by SPC for **3** in CH_3CN, λ_{ex} = 375 nm, λ_{em} = 510, 520 and 530 nm. The bottom panel of the figure corresponds to residuals between the fitted and experimental values.

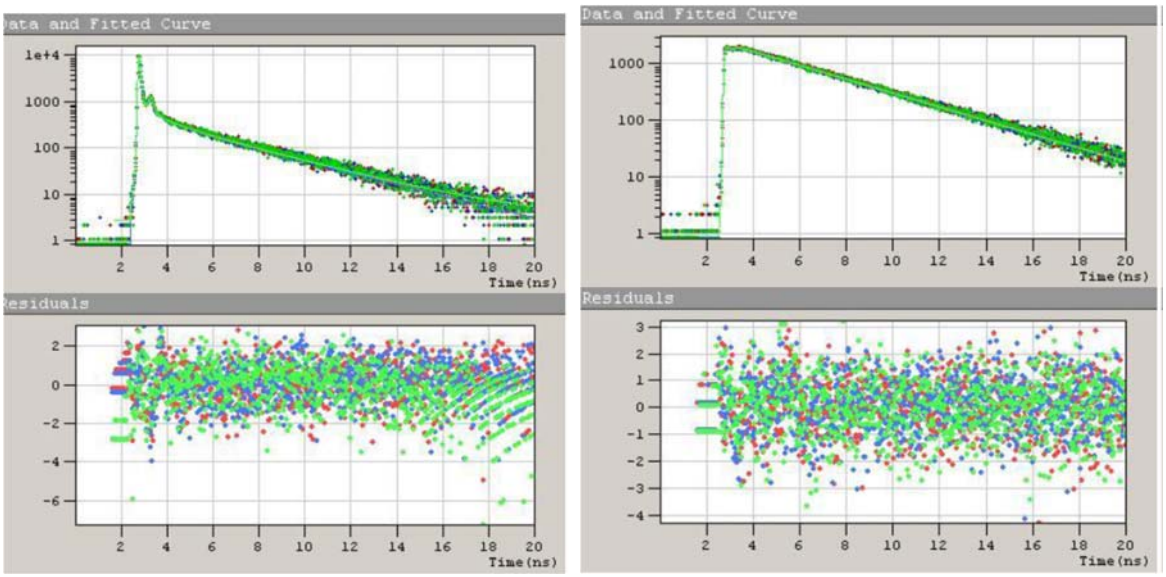

Figure S13. Global fitting of decays obtained by SPC for **4** in CH_3CN (left) and CH_3CN-H_2O (right), λ_{ex} = 375 nm, λ_{em} 510, 520 and 530 nm. The bottom panel of the figures correspond to residuals between the fitted and experimental values.

Table S2. Phototphysical properties of BODIPY dyes

	Φ (CH_3CN)[a]	Φ (CH_3CN-H_2O)[a]	τ (CH_3CN)/ns [b]	τ (CH_3CN-H_2O)/ns [b]
2	$(1.7\pm 0.3)\times10^{-3}$	$(9.5\pm 0.5)\times10^{-3}$	0.01 (13%) 0.13 ± 0.01 (25%) 1.2 ± 0.1 (8%) 11 ± 1 (54%)	0.18 (40%) 3.5 (20%) 15.3 (40%)
3	0.12 ± 0.02	0.25 ± 0.02	0.04 (7%) 3.39 ± 0.02 (93 %)	0.50 ± 0.03 (5%) 3.54 ± 0.01 (95%)
4	0.013±0.001	0.30 ± 0.03	0.04 (46%) 1.0 ± 0.1 (7%) 3.4 ± 0.2 (47%)	0.13 ± 0.01 (1%) 3.57 ± 0.01 (99%)
9	0.62 ± 0.04	0.11 ± 0.03	3.50 ± 0.02	0.16 ± 0.05 (5%) 0.90 ± 0.05 (95%)

[a] Quantum yield of fluorescence was measured using rhodamine 6G in CH_3OH as a reference (Φ_f = 0.86).5

[b] Measured by single photon counting (SPC). The contribution of different components are reported in parenthesis.

The unsubstituted BODIPY derivatives (**1** and **2**) compared to CH_3-substituted (**3** and **4)** are less fluorescent, probably due to a torsional motion between the two aromatic fragments leading

to the relaxation from S_1 (see computational part). The methyl-substituted phenol not bearing the methalamino group (**9**, see synthetic procedures, Scheme S7) is highly fluorescent in non-aqueous solvent ($\Phi_f = 0.62$), whereas in the presence of H_2O, the fluorescence is quenched most probably due to excited state proton transfer ESPT to solvent. ESPT is also indicated by SPC measurements, where a single exponential fluorescence decay was observed in CH_3CN solution, and a sum of two exponentials in CH_3CN-H_2O, probably corresponding to the phenol and phenolate emission. Introduction of the methylamino group into phenol (comparison of BODIPY **3** and **9**) results in fluorescence quenching due to excited state intramolecular proton transfer (ESIPT) from the phenolic OH to the amine nitrogen. ESIPT is manifested also in time-resolved fluorescence where fluorescence decay was fit to a sum of two exponentials. In nonaqueous solutions the Φ_f for salts **2** and **4** are also low, probably due to efficient non-radiative deactivation from S_1 imposed by BODIPY ring puckering (see computational part). However, in aqueous solvent **4** exhibits a reasonable Φ_f of 0.25-0.30.

3. Laser Flash Photolysis (LFP)

All LFP studies were performed on a system previously described[6] using as an excitation source a pulsed Nd:YAG laser at 355 nm (<50 mJ per pulse), with a pulse width of 10 ns. For the excitation in the visible region, the YAG 355 beam was used to pump an OPO that was set to the wavelength of 500 nm. Static cells (7 mm × 7 mm) were used and the solutions were purged with nitrogen or oxygen for 20 min prior to performing the measurements. Absorbances at the excitation wavelength were ~ 0.3-0.5. For the collection of decays at long time scales, a modification of the setup was used, wherein the probing light beam from the Xe-lamp was not pulsed, as previously described.[7]

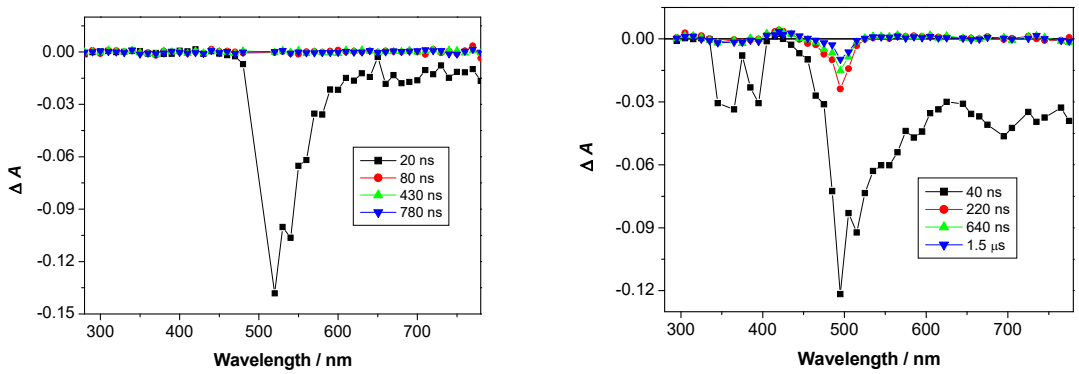

Figure S14. Transient absorption spectra for a N_2-purged CH_3CN solution of **2**, excited at 500 nm (left) and 355 nm (right).

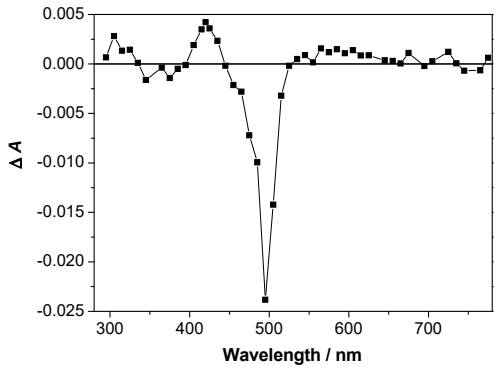

Figure S15. Transient absorption spectrum for a N_2-purged CH_3CN solution of **2** with a delay of 200 ns after the laser pulse (355 nm).

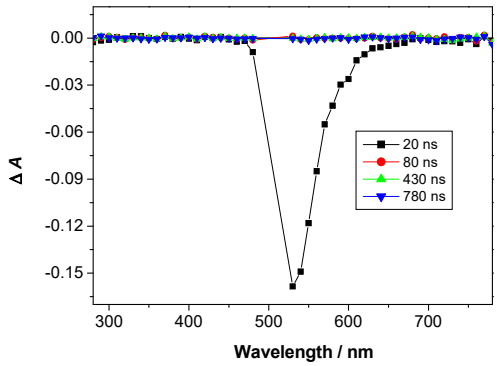

Figure S16. Transient absorption spectra for a N_2-purged CH_3CN solution of **3**, excited at 500 nm.

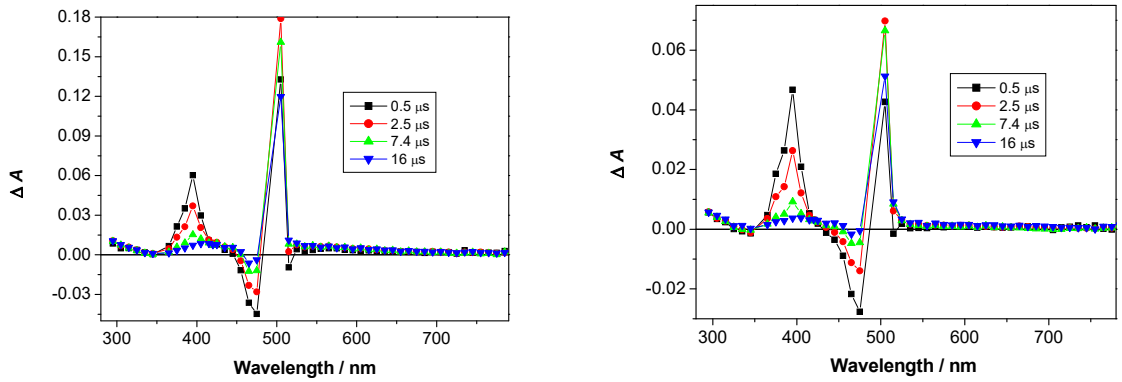

Figure S17. Transient absorption spectra for a N_2-purged (left) and O_2-purged CH_3CN solutions of **3**, excited at 355 nm.

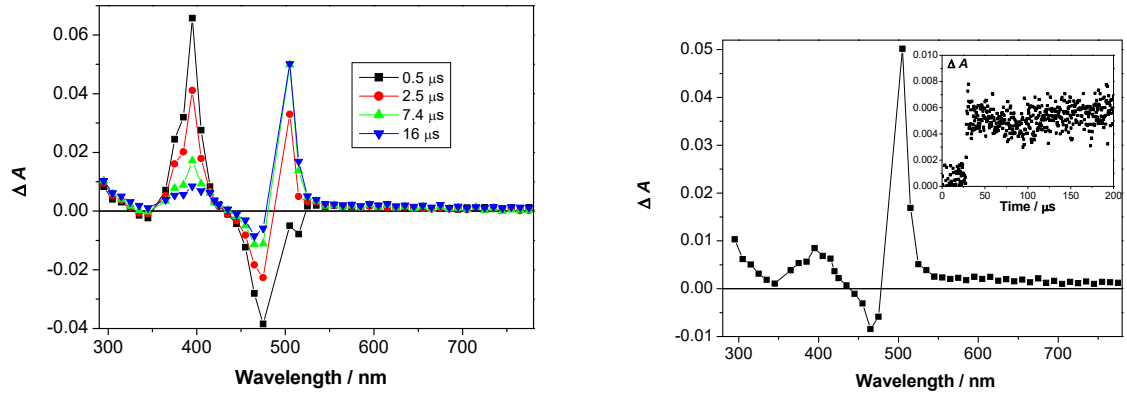

Figure S18. Transient absorption spectra for a O_2-purged CH_3CN-H_2O (1:1) solution of **3**, excited at 355 nm (left); and transient spectrum 16 μs after the laser pulse (right, inset: decay at 420 nm).

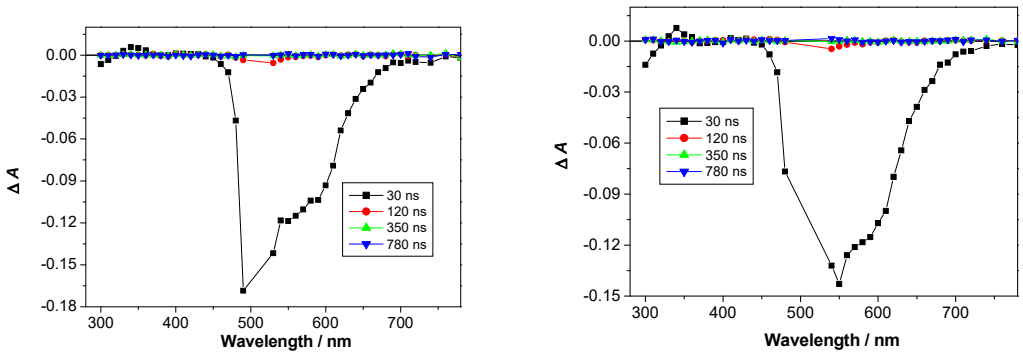

Figure S19. Transient absorption spectra for a N_2-purged CH_3CN (left) and CH_3CN-H_2O (1:1, right) solutions of **4**, excited at 500 nm.

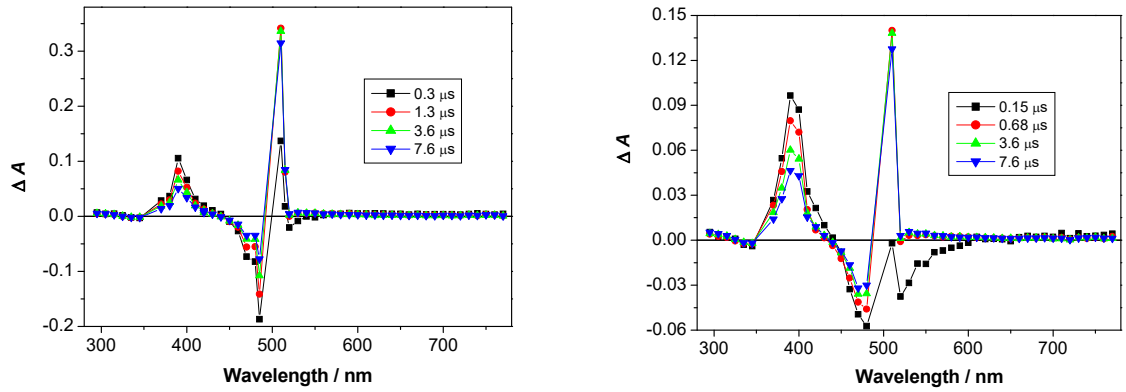

Figure S20. Transient absorption spectra for a N_2-purged (left) and O_2-purged CH_3CN solutions of **4**, excited at 355 nm.

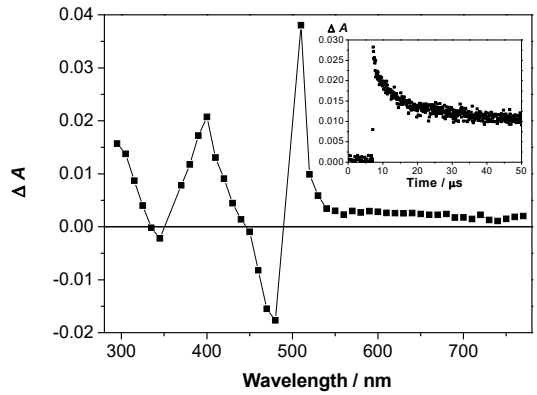

Figure S21. Transient absorption spectrum for a O_2-purged CH_3CN-H_2O (1:1) solution of **4**, excited at 355 nm, 15 μs after the laser flash (inset: decay at 410 nm).

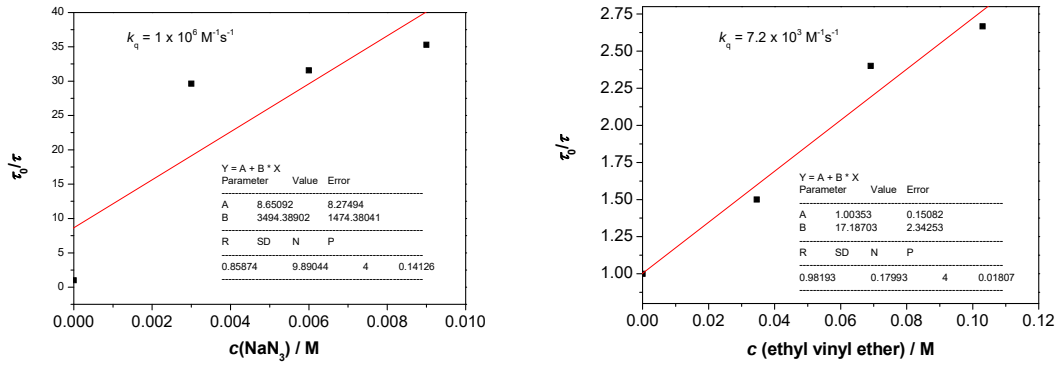

Figure S22. Stern-Vomer plots for the quenching of the transient assigned to QM (lifetime 2.4 ± 0.5 ms) at 420 nm with NaN_3 (left) and, ethyl vinyl ether (EVE).

4. Computations

The ground state geometries of BODIPY derivative **1** and its protonated form **1H**$^+$ as a model molecule for compound **2** were optimized at the PBE0/6-311G(2d,p) level of theory. Vibrational analyses were performed to verify the true minimum nature. Several orientations of the substituent group -$CH_2N(CH_3)_2$ were tested and the lowest energy structure was further used for the calculations of the excited-state properties. The vertical excitation energies and their oscillator strengths for 40 roots were calculated by means of the time-dependent functional theory (TD-DFT)[8] using different functionals: PBE0,[9] BMK,[10] CAM-B3LYP[11] and M062X.[12] For a recent review on the performance of different density functionals for calculation of the excitation energies in different molecules see ref. [13] All single point calculations of vertical excited energies have been performed by using 6-311+G(2d,p) basis set. Simulation of spectra from the calculated excitation energies and oscillator strengths was conducted by simple convolution fit with Gaussian functions with a half-width of 0.4 eV by using in-house created Perl script written by Dr. Mario Barbatti during our recent collaboration.[14] The DFT and TDDFT electronic data were obtained using Gaussian09 program [15] while Vega-ZZ[16] and Molden[17] programs were used for visualization and geometry manipulations.

A search for stationary points on the potential energy surface of the first excited singlet state of molecule **1** has been conducted using the PBE0 and BMK functional. The 6-311G(2d,p) basis set was used for optimizations and harmonic vibrational frequency analyses. Both methods revealed that two minima **1a** and **1b** could be found. In the case of **1a**, fully optimized scan along deamination reaction coordinate (C-N bond-dissociation and formation of quinonemethide **QM1**) in the first excited state were performed using the PBE0/6-311G(2d,p) level of theory. Furthermore, to complete the picture, quinonemethide structures **QM1** were independently optimized in the ground and in the first excited state.

In an attempt to optimize **1H**$^+$ structure in the first excited state it appears that the evolution of the system away from the Franck-Condon point on the S_1 PES lead toward structures with a very deformed BODIPY moiety and to a small S_0/S_1 energy gap where TD-DFT breaks down. It is an indication of a possible conical intersection on that path reachable without any energy barrier. Further theoretical investigation into that direction are prevented by the nature of the method used in this study. We are well aware that considerably higher levels of calculation of molecules on a conical intersection seam exist, but the size of the model molecules herein precludes the use of these higher level of calculations in the present study.

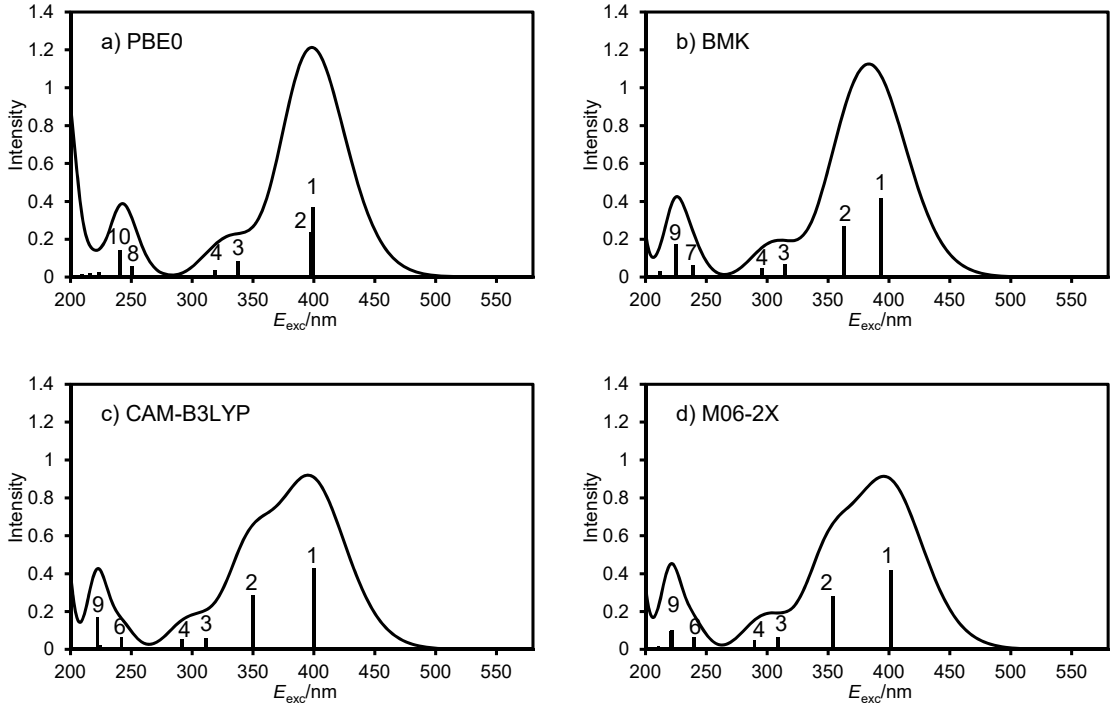

Figure S23. Comparison between the simulated UV-Vis spectra of **1** calculated at TD DFT level of theory using different density functionals: (a) PBE0, (b) BMK (c) CAM-B3LYP and (d) M06-2X. Pople type 6-311+G(2d,p) basis set was used in all calculations.

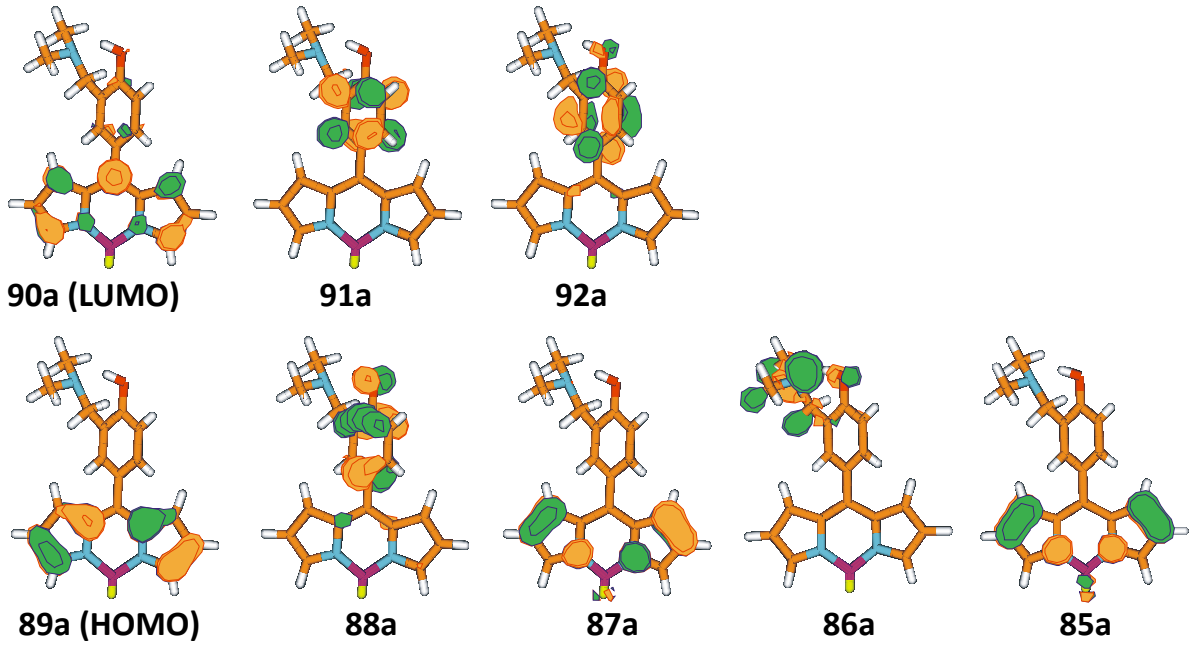

Figure S24. Selected Kohn-Sham orbitals of **1** at the PBE0/6-311+G(2d,p)//PBE0/6-311G(2d,p) level of theory.

Table S3. TD-DFT calculated vertical exitation energies (E_{exc}), oscilator strenght (f) and leading configurations for **1** at the PBE0/6-311+G(2d,p)//PBE0/6-311G(2d,p) level of theory.

Root	E_{exc}/eV	f	Leading configuration		Weight
1	3.108	0.3700	Singlet-A	89 -> 90	0.68245
2	3.116	0.2365	Singlet-A	88 -> 90	0.70022
3	3.674	0.0819	Singlet-A	87 -> 90	0.67924
4	3.888	0.0355	Singlet-A	85 -> 90	0.69594
5	3.976	0.0050	Singlet-A	84 -> 90	0.51054
6	4.129	0.0008	Singlet-A	86 -> 90	0.51116
7	4.752	0.0077	Singlet-A	89 -> 91	0.70465
8	4.939	0.0583	Singlet-A	88 -> 91	0.64577
9	5.072	0.0096	Singlet-A	89 -> 92	0.67925
10	5.154	0.1438	Singlet-A	83 -> 90	0.66025
11	5.513	0.0018	Singlet-A	89 -> 93	0.62814
12	5.533	0.0012	Singlet-A	82 -> 90	0.70092
13	5.554	0.0273	Singlet-A	88 -> 92	0.61911
14	5.716	0.0043	Singlet-A	88 -> 93	0.49673
15	5.739	0.0204	Singlet-A	86 -> 91	0.50552
16	5.864	0.0014	Singlet-A	89 -> 94	0.53462
17	5.925	0.0174	Singlet-A	87 -> 91	0.68249
18	5.984	0.0055	Singlet-A	89 -> 95	0.56669
19	6.019	0.0001	Singlet-A	81 -> 90	0.66293
20	6.094	0.0052	Singlet-A	86 -> 92	0.63101
21	6.125	0.0032	Singlet-A	89 -> 96	0.64832
22	6.138	0.0020	Singlet-A	85 -> 91	0.68008
23	6.148	0.0037	Singlet-A	88 -> 94	0.63598
24	6.170	0.0302	Singlet-A	80 -> 90	0.68665
25	6.206	0.2184	Singlet-A	89 -> 97	0.51105
26	6.229	0.0217	Singlet-A	87 -> 92	0.55266
27	6.241	0.0003	Singlet-A	88 -> 95	0.56168
28	6.263	0.0036	Singlet-A	78 -> 90	0.65053
29	6.320	0.0130	Singlet-A	88 -> 96	0.44746

30	6.336	0.0066	Singlet-A	88 -> 96	0.43489
31	6.354	0.0297	Singlet-A	86 -> 93	0.65504
32	6.368	0.0195	Singlet-A	89 -> 99	0.51147
33	6.419	0.0078	Singlet-A	89 ->100	0.43907
34	6.460	0.0604	Singlet-A	85 -> 92	0.61235
35	6.484	0.0088	Singlet-A	89 ->102	0.35060
36	6.512	0.0153	Singlet-A	79 -> 90	0.37573
37	6.544	0.1277	Singlet-A	79 -> 90	0.42095
38	6.549	0.1075	Singlet-A	88 -> 97	0.44826
39	6.570	0.0392	Singlet-A	88 -> 97	0.35463
40	6.594	0.0755	Singlet-A	84 -> 91	0.35046

Table S4. TD-DFT calculated vertical exitation energies (E_{exc}), oscilator strenght (f) and leading configurations for **1** at the BMK/6-311+G(2d,p)//PBE0/6-311G(2d,p) level of theory.

Root	E_{exc}/eV	f	Leading configuration		Weight
1	3.150	0.4181	Singlet-A	89 -> 90	0.69345
2	3.410	0.2671	Singlet-A	88 -> 90	0.70058
3	3.941	0.0687	Singlet-A	87 -> 90	0.68666
4	4.194	0.0453	Singlet-A	85 -> 90	0.69652
5	4.422	0.0032	Singlet-A	84 -> 90	0.59173
6	4.872	0.0005	Singlet-A	86 -> 90	0.60462
7	5.179	0.0643	Singlet-A	88 -> 91	0.63714
8	5.323	0.0126	Singlet-A	89 -> 91	0.70151
9	5.513	0.1723	Singlet-A	83 -> 90	0.66713
10	5.586	0.0076	Singlet-A	89 -> 92	0.69153
11	5.841	0.0333	Singlet-A	88 -> 92	0.62088
12	5.943	0.0013	Singlet-A	82 -> 90	0.67432
13	6.200	0.0005	Singlet-A	89 -> 93	0.47964
14	6.328	0.0168	Singlet-A	86 -> 91	0.64115
15	6.388	0.0092	Singlet-A	88 -> 93	0.53469
16	6.487	0.0035	Singlet-A	89 -> 95	0.53566
17	6.514	0.2756	Singlet-A	89 ->100	0.45167
18	6.553	0.0016	Singlet-A	81 -> 90	0.58320
19	6.590	0.0050	Singlet-A	79 -> 90	0.60087
20	6.674	0.0469	Singlet-A	89 -> 93	0.33880
21	6.685	0.0612	Singlet-A	87 -> 91	0.52895
22	6.727	0.0375	Singlet-A	86 -> 92	0.52224
23	6.755	0.0065	Singlet-A	89 -> 96	0.46680
24	6.815	0.0017	Singlet-A	89 -> 97	0.37570
25	6.827	0.1896	Singlet-A	84 -> 92	0.42178
26	6.832	0.0588	Singlet-A	88 -> 94	0.46103
27	6.861	0.0470	Singlet-A	89 ->105	0.34818
28	6.900	0.3386	Singlet-A	84 -> 91	0.48687
29	6.933	0.0091	Singlet-A	85 -> 91	0.63440
30	6.965	0.0013	Singlet-A	88 -> 96	0.38052
31	7.000	0.0026	Singlet-A	89 -> 98	0.30786
32	7.003	0.0088	Singlet-A	80 -> 90	0.35428
33	7.013	0.0036	Singlet-A	88 -> 96	0.33940
34	7.057	0.0086	Singlet-A	89 ->101	0.36413
35	7.063	0.1066	Singlet-A	87 -> 92	0.35635
36	7.089	0.0122	Singlet-A	75 -> 90	0.47729
37	7.092	0.0403	Singlet-A	86 -> 93	0.35058
38	7.107	0.0146	Singlet-A	86 -> 93	0.33299
39	7.198	0.0032	Singlet-A	78 -> 90	0.65101
40	7.217	0.0310	Singlet-A	85 -> 92	0.50262

Table S5. TD-DFT calculated vertical exitation energies (E_{exc}), oscilator strenght (f) and leading configurations for **1** at the CAM-B3LYP/6-311+G(2d,p)//PBE0/6-311G(2d,p) level of theory.

Root	E_{exc}/eV	f	Leading configuration		Weight
1	3.102	0.4304	Singlet-A	89 -> 90	0.69405
2	3.541	0.2877	Singlet-A	88 -> 90	0.69455
3	3.984	0.0577	Singlet-A	87 -> 90	0.68337
4	4.251	0.0526	Singlet-A	85 -> 90	0.69143
5	4.564	0.0032	Singlet-A	84 -> 90	0.53891
6	5.124	0.0641	Singlet-A	88 -> 91	0.54313
7	5.378	0.0024	Singlet-A	86 -> 90	0.56555
8	5.521	0.0251	Singlet-A	89 -> 91	0.63484
9	5.577	0.1723	Singlet-A	83 -> 90	0.64224
10	5.739	0.0076	Singlet-A	88 -> 93	0.47391
11	5.748	0.0069	Singlet-A	89 -> 93	0.52970
12	5.898	0.0007	Singlet-A	89 -> 94	0.38895
13	6.000	0.0036	Singlet-A	88 -> 92	0.37715
14	6.004	0.0012	Singlet-A	82 -> 90	0.68154
15	6.229	0.0082	Singlet-A	89 -> 95	0.51327
16	6.391	0.2251	Singlet-A	89 ->104	0.47223
17	6.409	0.0095	Singlet-A	86 -> 91	0.48952
18	6.485	0.0307	Singlet-A	89 -> 98	0.36186
19	6.507	0.0070	Singlet-A	89 ->100	0.36500
20	6.559	0.0241	Singlet-A	88 -> 94	0.45575
21	6.580	0.0017	Singlet-A	89 -> 99	0.36416
22	6.607	0.0319	Singlet-A	86 -> 92	0.33041
23	6.622	0.0361	Singlet-A	86 -> 92	0.40126
24	6.651	0.1016	Singlet-A	84 -> 93	0.28317
25	6.711	0.0061	Singlet-A	78 -> 90	0.50980
26	6.751	0.3033	Singlet-A	84 -> 91	0.44087
27	6.768	0.0719	Singlet-A	81 -> 90	0.35697
28	6.785	0.0175	Singlet-A	81 -> 90	0.38809
29	6.811	0.1109	Singlet-A	88 -> 96	0.24136
30	6.837	0.1082	Singlet-A	89 ->109	0.42888
31	6.888	0.0385	Singlet-A	89 -> 94	0.23344
32	6.933	0.0078	Singlet-A	89 -> 94	0.26923
33	6.941	0.0604	Singlet-A	87 -> 94	0.32268
34	6.996	0.0381	Singlet-A	87 -> 91	0.36124
35	7.006	0.0069	Singlet-A	88 -> 99	0.32377
36	7.028	0.0090	Singlet-A	86 -> 93	0.40280
37	7.044	0.0010	Singlet-A	80 -> 90	0.61581
38	7.065	0.0220	Singlet-A	84 -> 93	0.32621
39	7.121	0.0295	Singlet-A	85 -> 91	0.24973
40	7.192	0.0087	Singlet-A	89 ->105	0.23433

Table S6. TD-DFT calculated vertical exitation energies (E_{exc}), oscilator strenght (f) and leading configurations for **1** at the M06-2X/6-311+G(2d,p)//PBE0/6-311G(2d,p) level of theory.

Root	E_{exc}/eV	f	Leading configuration		Weight
1	3.087	0.4184	Singlet-A	89 -> 90	0.69456
2	3.504	0.2832	Singlet-A	88 -> 90	0.69715
3	4.018	0.0652	Singlet-A	87 -> 90	0.68339
4	4.278	0.0491	Singlet-A	85 -> 90	0.68916
5	4.558	0.0029	Singlet-A	84 -> 90	0.48559
6	5.168	0.0629	Singlet-A	88 -> 92	0.50266
7	5.283	0.0042	Singlet-A	84 -> 90	0.48618
8	5.407	0.0113	Singlet-A	89 -> 92	0.47729
9	5.591	0.1031	Singlet-A	83 -> 90	0.45944
10	5.613	0.0960	Singlet-A	83 -> 90	0.45954
11	5.730	0.0029	Singlet-A	89 -> 94	0.54900

12	5.769	0.0061	Singlet-A	88 -> 91	0.41218
13	5.880	0.0169	Singlet-A	88 -> 94	0.49082
14	6.000	0.0051	Singlet-A	89 -> 95	0.40299
15	6.054	0.0011	Singlet-A	81 -> 90	0.50987
16	6.194	0.0145	Singlet-A	89 -> 98	0.39418
17	6.210	0.0058	Singlet-A	89 -> 96	0.39757
18	6.338	0.0035	Singlet-A	89 -> 99	0.38481
19	6.373	0.0053	Singlet-A	88 -> 93	0.54527
20	6.398	0.0027	Singlet-A	88 -> 95	0.49445
21	6.413	0.0191	Singlet-A	86 -> 91	0.45408
22	6.455	0.0406	Singlet-A	88 -> 96	0.48718
23	6.475	0.1593	Singlet-A	89 ->107	0.44568
24	6.495	0.0213	Singlet-A	89 -> 97	0.35917
25	6.563	0.0219	Singlet-A	89 -> 93	0.39071
26	6.593	0.0223	Singlet-A	79 -> 90	0.58843
27	6.612	0.0832	Singlet-A	86 -> 92	0.48314
28	6.641	0.0630	Singlet-A	89 -> 99	0.27357
29	6.699	0.0362	Singlet-A	81 -> 90	0.37788
30	6.722	0.0879	Singlet-A	84 -> 92	0.32358
31	6.744	0.0643	Singlet-A	87 -> 91	0.40405
32	6.795	0.0510	Singlet-A	88 -> 99	0.31905
33	6.804	0.1820	Singlet-A	84 -> 91	0.24861
34	6.853	0.0238	Singlet-A	89 ->111	0.33854
35	6.858	0.0494	Singlet-A	89 ->111	0.30920
36	6.883	0.0564	Singlet-A	89 ->111	0.25618
37	6.907	0.0954	Singlet-A	87 -> 92	0.26704
38	6.937	0.0016	Singlet-A	89 ->102	0.33656
39	6.967	0.0194	Singlet-A	88 ->100	0.31698
40	6.991	0.0398	Singlet-A	84 -> 94	0.31886

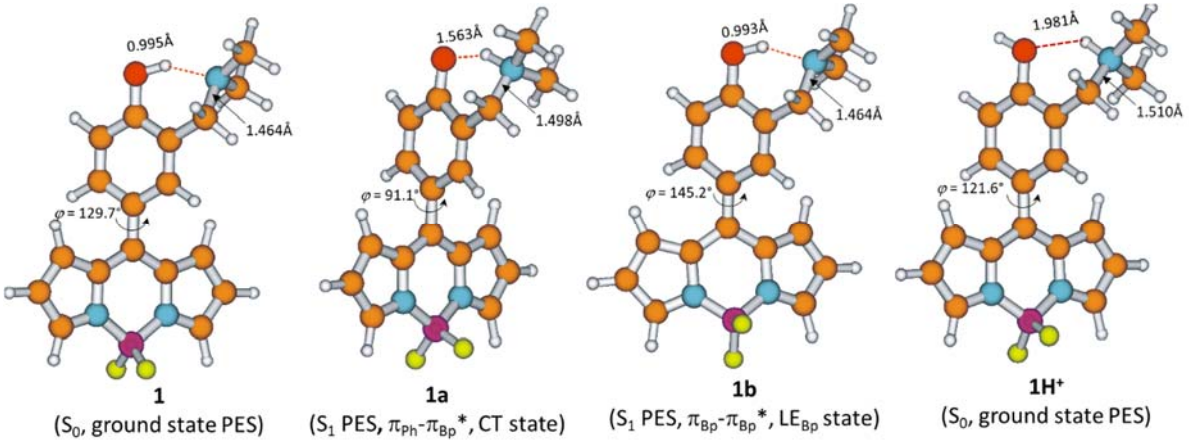

Figure S25. Optimized geometries of BODIPY **1** at the S_0 and S_1 potential energy surface at the PBE0/6-311G(2d,p) level of theory. Its protonated form in the ground state was shown as well.

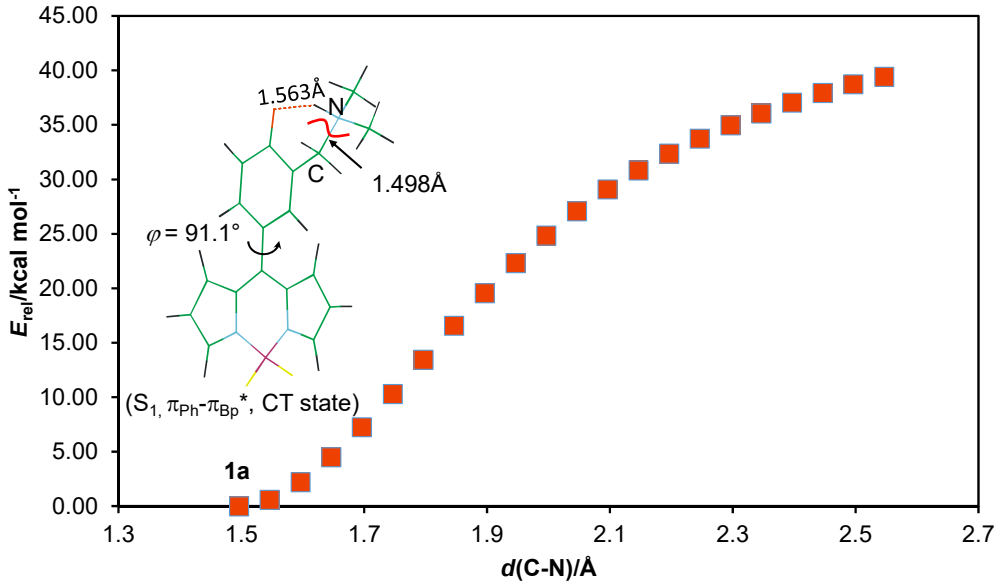

Figure S26. Potential energy surface scan for the deamination process (cleavage of the C-N bond) in the first excited state of bodipy **1** and formation of QM. Relative energies are given with respect to the **1a** minimum in the CT excited state.

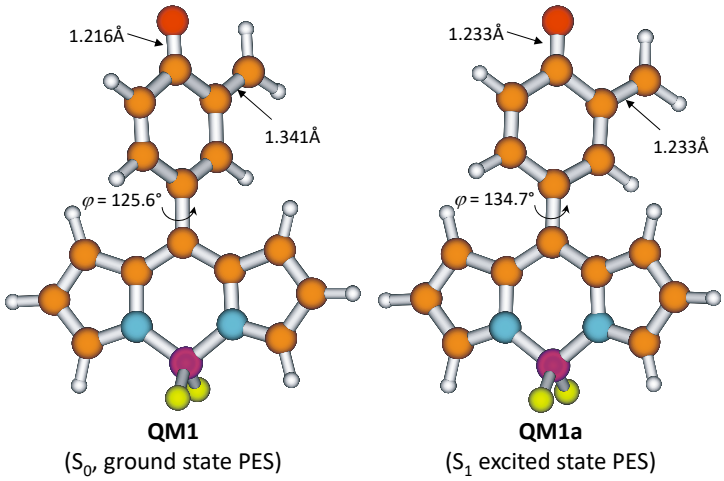

Figure S27. Optimized geometries of **QM1** in the S_0 and **QM1a** in the S_1 state calculated at the PBE0/6-311G(2d,p) level of theory.

Table S7. Total electronic energies for ground state (S_0) and the first excited state (S_1), zero point vibrational energies (ZVPE) and number of imaginary frequencies calculated at PBE0/6-311G(2d,p) level of theory. BMK results for BODIPY **1** are given as well.

Structure	Opt. state	E_{tot} (S_0)/a.u.	E_{tot} (S_1)/a.u.	ZPVE/a.u.	N_{Imag}	E_{exc}/kcal mol^{-1}
			PBE0/6-311G(2d,p)			
1	S_0	-1159.95731	-1159.84201	0.341022	0	72.35 (Vertical)
1a	S_1	-1159.92429	-1159.86461	0.339582	0	58.18 (Adiabatic)
1b	S_1	-1159.94723	-1159.84597	0.336664	0	69.88 (Adiabatic)
QM1	S_0	-1024.85055	-1024.75671	0.242419	0	58.90 (Vertical)
QM1a	S_1	-1024.84140	-1024.76595	0.239689	0	53.09(Adiabatic)
DMA	S_0	-135.033831			0	
1H$^+$	S_0	-1160.33006	-1160.21859	0.355496	0	69.95(Vertical)
			BMK/6-311G(2d,p)			
1	S_0	-1160.58956				
1a	S_1	-1160.55144	-1160.48546			65.33 (Vertical)
1b	S_1	-1160.58512	-1160.47635			71.05 (Adiabatic)

Table S8. Cartesian geometries (Å) for stationary points in the ground (S_0) and the first excited singlet state (S_1) calculated at the PBE0/6-311G(2d,p) level of theory

1 (S_0)

B	3.923628	0.569567	0.203024
N	2.714791	1.500361	-0.105974
C	1.401987	1.106399	-0.275823
C	1.022189	-0.236797	-0.149899
C	1.995382	-1.205881	0.122415
N	3.329285	-0.868393	0.249204
C	2.788534	2.810226	-0.336779
C	0.651440	2.245379	-0.639030
C	-0.383250	-0.624371	-0.305025
C	1.874206	-2.592596	0.361147
C	4.010855	-1.975083	0.539038
C	3.144921	-3.074135	0.611616
C	1.525005	3.316541	-0.666256
F	4.858980	0.668154	-0.800831
F	4.469807	0.887933	1.425396
H	3.735885	3.325454	-0.271031
H	1.299538	4.343534	-0.908905
H	-0.401329	2.250849	-0.874291
H	5.079247	-1.934833	0.694760
H	3.430937	-4.090276	0.835179
H	0.949576	-3.148380	0.363660
C	-0.756685	-1.666514	-1.159799
C	-2.082101	-2.013866	-1.318985
C	-3.076392	-1.349434	-0.602716
C	-2.721878	-0.318438	0.285784
C	-1.390334	0.039646	0.399690
H	0.005185	-2.176765	-1.738137
H	-2.378878	-2.797094	-2.006823
O	-4.352916	-1.710700	-0.777679
C	-3.774842	0.313971	1.154383
H	-1.115694	0.830399	1.091283
H	-3.383510	1.236909	1.612573
N	-5.024047	0.563502	0.433414

H	-4.015770	-0.370810	1.976453
C	-6.110265	0.863457	1.348739
C	-4.868993	1.614120	-0.559792
H	-7.036783	0.996816	0.787123
H	-6.247644	0.035025	2.046547
H	-5.922511	1.781177	1.928604
H	-5.790795	1.712818	-1.135866
H	-4.639762	2.586282	-0.094962
H	-4.059295	1.359019	-1.245390
H	-4.901170	-0.991177	-0.364320

1H$^+$ (S_0)

B	3.862835	0.614734	0.361781
N	2.704281	1.491719	-0.214712
C	1.401865	1.076005	-0.398704
C	1.043051	-0.260829	-0.212809
C	2.003125	-1.214030	0.113884
N	3.328005	-0.853923	0.277638
C	2.781716	2.776219	-0.548281
C	0.656440	2.178835	-0.877628
C	-0.369088	-0.661378	-0.372608
C	1.903289	-2.613962	0.312886
C	4.022176	-1.951895	0.552079
C	3.174061	-3.074555	0.575352
C	1.525992	3.246180	-0.967610
F	4.987084	0.758122	-0.401737
F	4.073481	0.941904	1.676612
H	3.721677	3.305065	-0.482012
H	1.311140	4.246382	-1.310404
H	-0.385174	2.158406	-1.159974
H	5.086841	-1.898587	0.730411
H	3.480006	-4.090908	0.768550
H	0.995559	-3.196168	0.266366
C	-0.751486	-1.628228	-1.300739
C	-2.078776	-2.001570	-1.439618
C	-3.038422	-1.420965	-0.629423
C	-2.684911	-0.452925	0.312334
C	-1.353718	-0.075137	0.419295
H	-0.000419	-2.080147	-1.938255
H	-2.362639	-2.743553	-2.179771
O	-4.368699	-1.731055	-0.701662
C	-3.728545	0.094743	1.230247
H	-1.063713	0.666544	1.156825
H	-3.320271	0.854354	1.898422
N	-4.873860	0.729667	0.479167
H	-4.179316	-0.696935	1.833854
C	-6.010808	1.038150	1.381270
C	-4.449538	1.921302	-0.297075
H	-6.828501	1.455280	0.795438
H	-6.334726	0.122112	1.872821
H	-5.681690	1.763410	2.124757
H	-5.289390	2.272758	-0.894356
H	-4.139394	2.698459	0.401028
H	-3.617835	1.644651	-0.942092
H	-5.173514	0.003105	-0.183611
H	-4.515834	-2.437674	-1.339234

1a (S_1)

B	3.835686	0.286191	0.535840
N	2.872393	1.357892	-0.028639

C	1.564345	1.148563	-0.394054
C	1.033595	-0.155207	-0.397044
C	1.832325	-1.263086	-0.062488
N	3.144223	-1.078445	0.305135
C	3.137235	2.681668	-0.140499
C	1.000919	2.390210	-0.740902
C	-0.396722	-0.346826	-0.697566
C	1.561585	-2.643841	-0.048346
C	3.692149	-2.294093	0.541877
C	2.747078	-3.284250	0.332839
C	2.007760	3.350980	-0.578749
F	5.052388	0.331865	-0.125453
F	4.036403	0.495646	1.895740
H	4.117611	3.062139	0.101294
H	1.934797	4.411852	-0.767104
H	-0.004438	2.555655	-1.098958
H	4.724199	-2.374862	0.846307
H	2.910314	-4.346505	0.437901
H	0.624556	-3.111984	-0.310886
C	-0.862061	-0.568049	-2.006598
C	-2.197261	-0.699820	-2.275682
C	-3.165229	-0.611380	-1.223397
C	-2.678620	-0.426309	0.127883
C	-1.339194	-0.292191	0.353730
H	-0.131605	-0.615892	-2.804583
H	-2.576112	-0.845724	-3.280242
O	-4.408692	-0.658979	-1.461186
C	-3.673817	-0.453397	1.244081
H	-0.958003	-0.142122	1.358093
H	-3.270831	-0.032452	2.167359
N	-4.907047	0.300463	0.853341
H	-3.996269	-1.479406	1.444376
C	-6.073007	-0.056774	1.678575
C	-4.674252	1.758493	0.815980
H	-6.941315	0.502027	1.331984
H	-6.265416	-1.124430	1.581860
H	-5.871385	0.189046	2.722163
H	-5.541545	2.246130	0.373358
H	-4.518122	2.125220	1.831259
H	-3.790735	1.962290	0.213032
H	-5.021679	-0.055222	-0.156218

1b (S_1)

B	-3.726111	-0.737848	0.576380
N	-2.631037	-1.534960	-0.158557
C	-1.349940	-1.025166	-0.433280
C	-1.009764	0.352612	-0.192731
C	-2.113955	1.235393	-0.030623
N	-3.411554	0.715908	0.162312
C	-2.711438	-2.774747	-0.631925
C	-0.634353	-2.016771	-1.096623
C	0.371174	0.765145	-0.230942
C	-2.230020	2.631493	-0.079110
C	-4.277217	1.726940	0.190129
C	-3.585224	2.939628	0.047200
C	-1.482978	-3.127758	-1.216725
F	-4.974565	-1.106658	0.133631
F	-3.601190	-0.889081	1.940263
H	-3.623054	-3.344603	-0.534833

H	-1.249188	-4.081150	-1.666962
H	0.366630	-1.913997	-1.484031
H	-5.328548	1.544347	0.354468
H	-4.027529	3.924609	0.068418
H	-1.422888	3.336153	-0.182227
C	0.802376	1.977198	-0.803633
C	2.133461	2.332063	-0.820313
C	3.098259	1.505113	-0.247689
C	2.701013	0.291761	0.345420
C	1.367425	-0.062562	0.321705
H	0.088192	2.612703	-1.310656
H	2.460990	3.249382	-1.296342
O	4.384287	1.881811	-0.280064
C	3.714225	-0.546902	1.075823
H	1.067658	-0.990118	0.799842
H	3.298664	-1.546336	1.284451
N	4.990043	-0.636586	0.363583
H	3.927351	-0.082942	2.046368
C	6.034958	-1.170342	1.217453
C	4.867778	-1.409340	-0.861589
H	6.982991	-1.178548	0.676132
H	6.149395	-0.540334	2.101823
H	5.816915	-2.198779	1.547716
H	5.810711	-1.378009	-1.410736
H	4.615517	-2.462560	-0.658292
H	4.086503	-0.982279	-1.492377
H	4.910911	1.075787	-0.035862

QM1 (S_0)

B	-3.105764	0.086115	0.124303
N	-2.216457	-1.194461	0.103544
C	-0.835732	-1.225224	0.058119
C	-0.091850	-0.050882	-0.086555
C	-0.743334	1.179807	-0.196902
N	-2.119842	1.268287	-0.122942
C	-2.651777	-2.441421	0.267019
C	-0.424429	-2.568483	0.209338
C	1.377961	-0.106337	-0.134645
C	-0.237050	2.472510	-0.466255
C	-2.463194	2.538260	-0.321834
C	-1.320797	3.324359	-0.535144
C	-1.569107	-3.330687	0.332086
F	-4.038910	0.036861	-0.882215
F	-3.699550	0.217662	1.356906
H	-3.709919	-2.647556	0.339293
H	-1.636572	-4.399898	0.459902
H	0.597435	-2.915803	0.233139
H	-3.502963	2.832126	-0.314385
H	-1.312420	4.385123	-0.732187
H	0.802509	2.718919	-0.616286
C	2.034268	-0.982174	-1.093885
C	3.370501	-1.090924	-1.177981
C	4.255180	-0.336372	-0.292228
C	3.570954	0.561606	0.699407
C	2.129297	0.632906	0.711652
H	1.399956	-1.542387	-1.773534
H	3.848594	-1.730828	-1.910497
O	5.466351	-0.423563	-0.354038
C	4.326986	1.267979	1.552384

H	1.651856	1.274296	1.445703
H	3.885959	1.928724	2.290805
H	5.406542	1.178183	1.504951
QM1a (S_1)			
B	-3.117880	0.142362	0.176647
N	-2.261499	-1.158787	0.066460
C	-0.875016	-1.238731	0.009621
C	-0.054577	-0.096559	-0.148113
C	-0.719146	1.145795	-0.246178
N	-2.091125	1.285256	-0.076980
C	-2.734431	-2.380740	0.233245
C	-0.508605	-2.608172	0.165720
C	1.382731	-0.182566	-0.212064
C	-0.188636	2.424027	-0.587789
C	-2.401482	2.552799	-0.281356
C	-1.233864	3.304792	-0.593656
C	-1.666747	-3.322388	0.286823
F	-4.082555	0.159821	-0.792623
F	-3.643160	0.239439	1.435508
H	-3.796618	-2.551599	0.340636
H	-1.778036	-4.386514	0.424302
H	0.505147	-2.970649	0.193233
H	-3.429804	2.883277	-0.233506
H	-1.211656	4.358999	-0.821074
H	0.846034	2.611594	-0.822084
C	2.048023	-1.197541	-0.948317
C	3.411907	-1.281197	-0.949711
C	4.257861	-0.399364	-0.184251
C	3.555660	0.647036	0.605043
C	2.147088	0.721498	0.532398
H	1.470417	-1.856563	-1.588091
H	3.921428	-2.020354	-1.558033
O	5.487151	-0.495575	-0.174927
C	4.297843	1.505936	1.377415
H	1.646428	1.454829	1.158371
H	3.832193	2.277709	1.978415
H	5.374812	1.405686	1.378711
Dimethylamine (S_0)			
N	0.000029	0.565826	-0.150517
C	-1.202352	-0.221693	0.020346
C	1.202363	-0.221680	0.020346
H	-1.252365	-0.766993	0.979238
H	-2.082326	0.421000	-0.056089
H	-1.267533	-0.964348	-0.780976
H	1.253289	-0.765580	0.979984
H	1.266398	-0.965501	-0.779961
H	2.082439	0.420656	-0.057958
H	-0.000166	1.320224	0.525230

Table S9. Cartesian geometry (Å) for the last point in an attempt of the **1H**$^+$ optimization in the first excited state (S_1) calculated at the PBE0/6-311G(2d,p) level of theory.

1H$^+$ (S_1, unconverged due to small S_0/S_1 energy gap)			
B	3.528497	0.798320	0.796613
N	2.523337	1.585083	-0.080928
C	1.332500	0.991277	-0.519882

C	1.039623	-0.413635	-0.281366
C	2.191968	-1.224245	-0.185575
N	3.416274	-0.623591	0.175151
C	2.614022	2.800841	-0.598254
C	0.683742	1.895244	-1.345874
C	-0.325444	-0.848916	-0.253015
C	2.465557	-2.584349	-0.453838
C	4.370999	-1.535723	0.115126
C	3.822408	-2.775418	-0.278537
C	1.475827	3.054575	-1.387958
F	4.793579	1.284214	0.647153
F	3.090384	0.776029	2.095496
H	3.471157	3.427402	-0.400368
H	1.266271	3.973542	-1.914240
H	-0.231475	1.710238	-1.886367
H	5.386092	-1.288908	0.391519
H	4.370976	-3.698802	-0.386564
H	1.760907	-3.339930	-0.753949
C	-0.766864	-2.133457	-0.653201
C	-2.090262	-2.512537	-0.537416
C	-3.019005	-1.641498	0.001662
C	-2.626740	-0.355173	0.405884
C	-1.311037	0.028258	0.250039
H	-0.080970	-2.822092	-1.121661
H	-2.400095	-3.496236	-0.878310
O	-4.353115	-1.940407	0.147208
C	-3.623044	0.527792	1.077421
H	-1.006024	1.009727	0.597272
H	-3.204516	1.504837	1.322843
N	-4.838868	0.763287	0.208393
H	-4.009787	0.070303	1.991837
C	-5.935205	1.410573	0.967356
C	-4.509309	1.507355	-1.030339
H	-6.799556	1.532712	0.316258
H	-6.196983	0.783907	1.818556
H	-5.593819	2.385141	1.315286
H	-5.388923	1.538621	-1.671448
H	-4.211185	2.519948	-0.759342
H	-3.690098	0.998853	-1.535132
H	-5.139913	-0.185750	-0.053789
H	-4.518918	-2.853270	-0.108678

Table S10. Cartesian geometries (Å) for optimized structures of BODIPY **1** in the ground (S_0) and the first excited singlet state (S_1) calculated at the BMK/6-311G(2d,p) level of theory

1 (S_0)

B	3.900266	0.602740	0.253451
N	2.703077	1.504354	-0.143938
C	1.392867	1.095941	-0.300208
C	1.025688	-0.254679	-0.151736
C	2.017584	-1.212563	0.123245
N	3.346239	-0.847103	0.240874
C	2.775184	2.802900	-0.419388
C	0.631599	2.221848	-0.705328
C	-0.388173	-0.655733	-0.301429
C	1.930739	-2.611966	0.344603
C	4.060127	-1.936204	0.504621

C	3.220993	-3.066231	0.573062
C	1.504039	3.298286	-0.771533
F	4.913895	0.735098	-0.661844
F	4.332539	0.920984	1.517910
H	3.722935	3.320843	-0.367916
H	1.277173	4.314437	-1.055410
H	-0.420351	2.210287	-0.944575
H	5.129928	-1.867893	0.646543
H	3.537782	-4.077700	0.776185
H	1.022520	-3.194448	0.348946
C	-0.759811	-1.699503	-1.163595
C	-2.091282	-2.049351	-1.324396
C	-3.088343	-1.384151	-0.602333
C	-2.734768	-0.353777	0.295409
C	-1.398252	0.008213	0.411341
H	0.002874	-2.208731	-1.742416
H	-2.388834	-2.832557	-2.012671
O	-4.362404	-1.749131	-0.780229
C	-3.797599	0.280567	1.172277
H	-1.125264	0.798036	1.104684
H	-3.391428	1.183153	1.659341
N	-5.032343	0.584777	0.438719
H	-4.064079	-0.424436	1.969218
C	-6.110826	0.922589	1.359577
C	-4.824278	1.657220	-0.529084
H	-7.024659	1.118964	0.794283
H	-6.296204	0.085997	2.037249
H	-5.872574	1.816572	1.960031
H	-5.737614	1.811078	-1.107976
H	-4.556974	2.604914	-0.032062
H	-4.020065	1.386085	-1.215922
H	-4.926922	-1.044610	-0.387765

1a (S_1)

B	3.849081	0.289777	0.489733
N	2.861757	1.362402	-0.017005
C	1.556517	1.154788	-0.388455
C	1.023590	-0.160147	-0.394095
C	1.829878	-1.267332	-0.031443
N	3.137077	-1.070312	0.340811
C	3.128975	2.686058	-0.115317
C	0.987057	2.399563	-0.728950
C	-0.403012	-0.361922	-0.704291
C	1.554586	-2.650132	0.020976
C	3.686629	-2.275275	0.620340
C	2.745131	-3.280423	0.435533
C	1.999305	3.365698	-0.552648
F	5.009962	0.311722	-0.261582
F	4.161671	0.521628	1.820708
H	4.111103	3.059578	0.133049
H	1.929598	4.428516	-0.730193
H	-0.018429	2.564378	-1.086348
H	4.717276	-2.339321	0.935703
H	2.910744	-4.337856	0.577674
H	0.617657	-3.122909	-0.233610
C	-0.861012	-0.596710	-2.028005
C	-2.191748	-0.740938	-2.312091
C	-3.185478	-0.657341	-1.259664
C	-2.699403	-0.461519	0.108300

C	-1.363956	-0.310630	0.348315
H	-0.120176	-0.643192	-2.818030
H	-2.558560	-0.898244	-3.320247
O	-4.411640	-0.714696	-1.495185
C	-3.716763	-0.494990	1.217850
H	-0.992347	-0.153670	1.356198
H	-3.308555	-0.126816	2.162250
N	-4.919435	0.335698	0.859134
H	-4.090014	-1.513221	1.365222
C	-6.072549	0.052380	1.741424
C	-4.602986	1.784150	0.808699
H	-6.921125	0.660588	1.427585
H	-6.329242	-1.004368	1.666198
H	-5.800762	0.297568	2.770151
H	-5.470148	2.322894	0.426717
H	-4.361137	2.127878	1.816318
H	-3.748764	1.939958	0.150823
H	-5.108468	0.000596	-0.118229

1b (S_1)

B	3.827181	0.678762	0.443540
N	2.693742	1.512007	-0.178622
C	1.380600	1.065720	-0.389616
C	1.005719	-0.300363	-0.181436
C	2.074348	-1.227234	0.029004
N	3.399617	-0.777734	0.177234
C	2.779582	2.781019	-0.559979
C	0.642367	2.145039	-0.929233
C	-0.394571	-0.713038	-0.261092
C	2.094728	-2.641460	0.094451
C	4.196422	-1.833543	0.296481
C	3.426115	-3.022483	0.250338
C	1.517773	3.224493	-1.032518
F	5.021028	0.951188	-0.177993
F	3.911957	0.910949	1.797505
H	3.716823	3.314707	-0.488122
H	1.298619	4.214245	-1.405619
H	-0.387736	2.101839	-1.245112
H	5.260182	-1.705027	0.440225
H	3.812129	-4.027264	0.341113
H	1.234758	-3.288287	0.046817
C	-0.800575	-1.877200	-0.945216
C	-2.133588	-2.248856	-1.005074
C	-3.114350	-1.482149	-0.367357
C	-2.739198	-0.315091	0.333410
C	-1.401217	0.055831	0.357322
H	-0.064463	-2.464196	-1.481670
H	-2.447417	-3.128308	-1.556468
O	-4.390448	-1.882396	-0.442722
C	-3.777209	0.461601	1.122243
H	-1.116564	0.943012	0.915283
H	-3.362902	1.438746	1.423448
N	-5.041367	0.626010	0.393702
H	-4.008739	-0.090383	2.041431
C	-6.079422	1.149002	1.272458
C	-4.875136	1.485619	-0.774137
H	-7.019419	1.227572	0.721479
H	-6.228088	0.472534	2.117290
H	-5.819514	2.147356	1.663252

H	-5.815826	1.537388	-1.327076
H	-4.579020	2.508110	-0.484726
H	-4.107820	1.074025	-1.432679
H	-4.952456	-1.133365	-0.146876

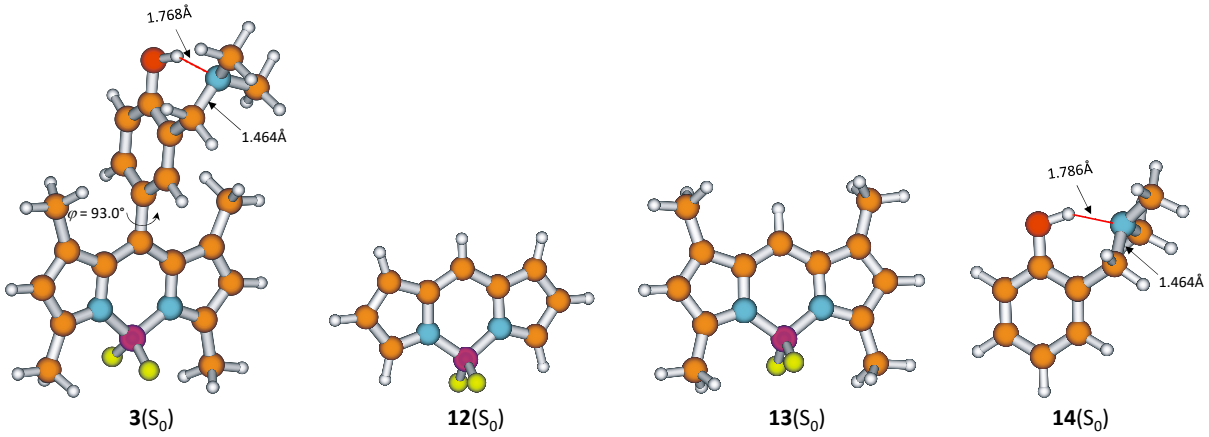

Figure S28. Optimized geometries of molecules **3** and **12-14** at the S_0 potential energy surface using PBE0/6-311G(2d,p) method.

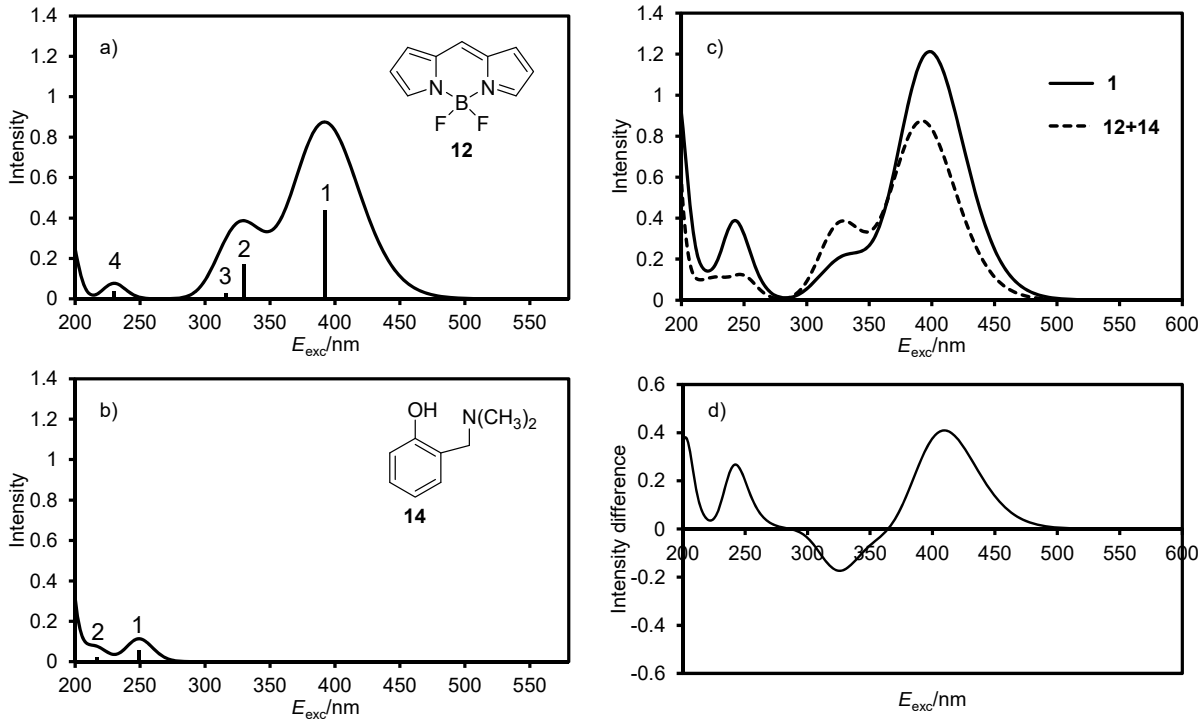

Figure S29. a) UV-Vis spectrum of molecule **12**, b) UV-Vis spectrum of molecule **14**, c) comparison between the UV-Vis spectra of BODIPY **1** with the sum of simulated spectra for **12** and **14**, d) Difference between the UV-Vis spectra for **1** and the sum of **12** and **14**. All calculations were performed at the TD-DFT level of theory using PBE0/6-311+G(2d,p)//PBE0/6-311G(2d,p).

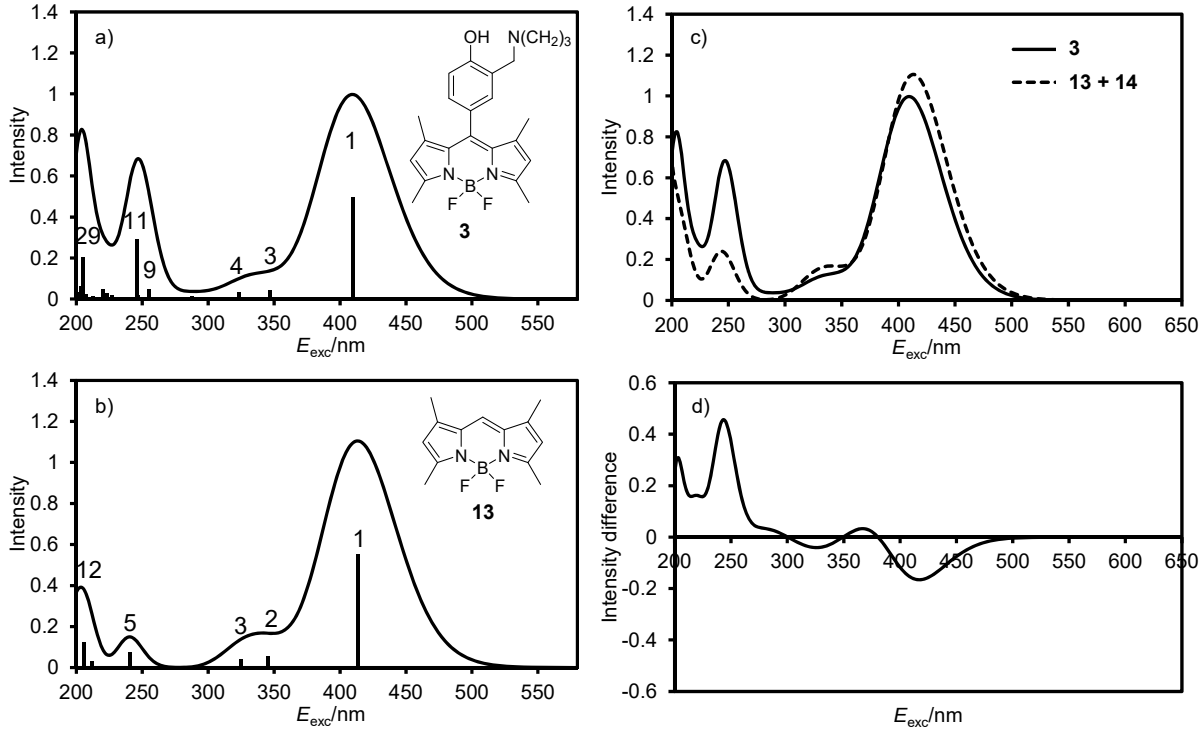

Figure S30. a) UV-Vis spectrum of molecule **3**, b) UV-Vis spectrum of molecule **13**, c) comparison between the UV-Vis spectra of BODIPY **3** with the sum of simulated spectra for **13** and **14**, d) Difference between the UV-Vis spectra for **3** and the sum of **13** and **14**. All calculations were performed at the TD-DFT level of theory using PBE0/6-311+G(2d,p)//PBE0/6-311G(2d,p).

Table S11. TD-DFT calculated vertical exitation energies (E_{exc}), oscilator strenght (f) and leading configurations for **3** at the PBE0/6-311+G(2d,p)//PBE0/6-311G(2d,p) level of theory.

Root	E_{exc}/eV	f	Leading configuration		Weight
1	3.027	0.4975	Singlet-A	105 ->106	0.70010
2	3.210	0.0023	Singlet-A	104 ->106	0.70410
3	3.577	0.0437	Singlet-A	103 ->106	0.69533
4	3.833	0.0300	Singlet-A	102 ->106	0.70415
5	4.249	0.0015	Singlet-A	100 ->106	0.56125
6	4.310	0.0132	Singlet-A	105 ->107	0.70195
7	4.461	0.0004	Singlet-A	101 ->106	0.56228
8	4.598	0.0007	Singlet-A	105 ->108	0.68760
9	4.856	0.0486	Singlet-A	104 ->107	0.65360
10	5.017	0.0159	Singlet-A	105 ->109	0.58966
11	5.034	0.2892	Singlet-A	99 ->106	0.64749
12	5.315	0.0005	Singlet-A	105 ->110	0.57568
13	5.441	0.0037	Singlet-A	105 ->111	0.64886
14	5.458	0.0052	Singlet-A	98 ->106	0.61204
15	5.460	0.0168	Singlet-A	104 ->108	0.51625
16	5.554	0.0276	Singlet-A	103 ->107	0.60594
17	5.588	0.0033	Singlet-A	105 ->112	0.66192
18	5.623	0.0462	Singlet-A	104 ->109	0.60500
19	5.684	0.0001	Singlet-A	105 ->113	0.63202
20	5.696	0.0085	Singlet-A	101 ->107	0.66344
21	5.744	0.0015	Singlet-A	102 ->107	0.54329
22	5.751	0.0032	Singlet-A	105 ->114	0.50691

23	5.800	0.0042	Singlet-A	105 ->115	0.59133
24	5.835	0.0115	Singlet-A	103 ->108	0.68235
25	5.979	0.0227	Singlet-A	105 ->116	0.50940
26	6.012	0.0136	Singlet-A	104 ->110	0.65300
27	6.015	0.0105	Singlet-A	101 ->108	0.64504
28	6.033	0.0048	Singlet-A	102 ->108	0.63120
29	6.049	0.2033	Singlet-A	105 ->117	0.47240
30	6.099	0.0634	Singlet-A	105 ->118	0.45985
31	6.103	0.0001	Singlet-A	97 ->106	0.66590
32	6.141	0.0082	Singlet-A	104 ->112	0.48815
33	6.142	0.0299	Singlet-A	105 ->119	0.50125
34	6.154	0.0067	Singlet-A	104 ->112	0.45481
35	6.194	0.0006	Singlet-A	103 ->109	0.55554
36	6.227	0.0030	Singlet-A	95 ->106	0.57852
37	6.230	0.0101	Singlet-A	105 ->120	0.52499
38	6.270	0.0317	Singlet-A	101 ->109	0.64143
39	6.278	0.0239	Singlet-A	105 ->121	0.39539
40	6.350	0.0020	Singlet-A	105 ->122	0.33057

Table S12. TD-DFT calculated vertical exitation energies (E_{exc}), oscilator strenght (f) and leading configurations for **13** at the PBE0/6-311+G(2d,p)//PBE0/6-311G(2d,p) level of theory.

Root	E_{exc}/eV	f	Leading configuration		Weight
1	3.160	0.4367	Singlet-A	49 -> 50	0.67341
2	3.761	0.1693	Singlet-A	48 -> 50	0.66830
3	3.923	0.0277	Singlet-A	47 -> 50	0.70350
4	5.391	0.0386	Singlet-A	46 -> 50	0.65703
5	5.514	0.0000	Singlet-A	45 -> 50	0.70283
6	5.722	0.0000	Singlet-A	49 -> 51	0.70099
7	6.126	0.0047	Singlet-A	49 -> 52	0.69989
8	6.159	0.0001	Singlet-A	44 -> 50	0.69150
9	6.274	0.0032	Singlet-A	43 -> 50	0.69233
10	6.294	0.0000	Singlet-A	49 -> 54	0.69718
11	6.355	0.1286	Singlet-A	49 -> 53	0.63169
12	6.443	0.0388	Singlet-A	49 -> 55	0.63900
13	6.598	0.0012	Singlet-A	42 -> 50	0.61454
14	6.627	0.0007	Singlet-A	49 -> 57	0.62934
15	6.664	0.0198	Singlet-A	49 -> 56	0.70139
16	6.718	0.0458	Singlet-A	49 -> 58	0.63845
17	6.752	0.0000	Singlet-A	41 -> 50	0.69296
18	6.876	0.0000	Singlet-A	49 -> 59	0.50057
19	6.891	0.0186	Singlet-A	49 -> 60	0.59773
20	6.904	0.0000	Singlet-A	48 -> 51	0.51079
21	7.017	0.0358	Singlet-A	47 -> 51	0.55442
22	7.132	0.0001	Singlet-A	40 -> 50	0.70091
23	7.174	0.0001	Singlet-A	39 -> 50	0.65145
24	7.222	0.0001	Singlet-A	49 -> 61	0.65308
25	7.337	0.0003	Singlet-A	38 -> 50	0.68748
26	7.351	0.0001	Singlet-A	49 -> 62	0.51807
27	7.388	0.0015	Singlet-A	48 -> 52	0.50100
28	7.394	0.0053	Singlet-A	49 -> 63	0.68435
29	7.420	0.0005	Singlet-A	49 -> 62	0.46926
30	7.484	0.0443	Singlet-A	49 -> 64	0.56100
31	7.498	0.0348	Singlet-A	49 -> 65	0.60610
32	7.530	0.5137	Singlet-A	47 -> 53	0.55373
33	7.613	0.0449	Singlet-A	48 -> 53	0.50808
34	7.639	0.0011	Singlet-A	48 -> 54	0.38814
35	7.659	0.0194	Singlet-A	48 -> 55	0.57456
36	7.696	0.0000	Singlet-A	47 -> 54	0.48389
37	7.825	0.0433	Singlet-A	48 -> 58	0.65401

38	7.877	0.0010	Singlet-A	48 -> 57	0.49468
39	7.956	0.0013	Singlet-A	48 -> 56	0.46757
40	7.982	0.0829	Singlet-A	47 -> 55	0.58843

Table S13. TD-DFT calculated vertical exitation energies (E_{exc}), oscilator strenght (f) and leading configurations for **12** at the PBE0/6-311+G(2d,p)//PBE0/6-311G(2d,p) level of theory.

Root	E_{exc}/eV	f	Leading configuration		Weight
1	2.999	0.5532	Singlet-A	65 -> 66	0.70124
2	3.587	0.0553	Singlet-A	64 -> 66	0.69492
3	3.815	0.0406	Singlet-A	63 -> 66	0.70423
4	5.029	0.0000	Singlet-A	65 -> 67	0.69909
5	5.152	0.0745	Singlet-A	62 -> 66	0.65439
6	5.459	0.0000	Singlet-A	61 -> 66	0.70252
7	5.478	0.0023	Singlet-A	65 -> 68	0.70111
8	5.615	0.0000	Singlet-A	65 -> 69	0.69508
9	5.844	0.0298	Singlet-A	65 -> 71	0.69739
10	5.925	0.0002	Singlet-A	65 -> 70	0.70018
11	6.003	0.0001	Singlet-A	65 -> 73	0.63114
12	6.014	0.1252	Singlet-A	65 -> 72	0.63687
13	6.149	0.0001	Singlet-A	65 -> 74	0.62444
14	6.257	0.0757	Singlet-A	65 -> 75	0.67743
15	6.279	0.0000	Singlet-A	64 -> 67	0.67033
16	6.325	0.0036	Singlet-A	59 -> 66	0.69594
17	6.388	0.0225	Singlet-A	65 -> 77	0.63987
18	6.391	0.0082	Singlet-A	65 -> 76	0.50536
19	6.419	0.0006	Singlet-A	60 -> 66	0.70039
20	6.443	0.0006	Singlet-A	65 -> 76	0.46260
21	6.557	0.0000	Singlet-A	65 -> 78	0.46513
22	6.558	0.0002	Singlet-A	65 -> 78	0.46094
23	6.696	0.0018	Singlet-A	57 -> 66	0.50731
24	6.732	0.0003	Singlet-A	65 -> 79	0.67304
25	6.785	0.0070	Singlet-A	64 -> 68	0.54403
26	6.786	0.0092	Singlet-A	65 -> 80	0.58005
27	6.810	0.0002	Singlet-A	64 -> 69	0.54733
28	6.854	0.0012	Singlet-A	55 -> 66	0.49870
29	6.858	0.0017	Singlet-A	58 -> 66	0.45536
30	7.007	0.0088	Singlet-A	63 -> 68	0.45689
31	7.017	0.0189	Singlet-A	64 -> 72	0.53132
32	7.027	0.2474	Singlet-A	64 -> 71	0.54532
33	7.040	0.0086	Singlet-A	63 -> 69	0.48677
34	7.060	0.0005	Singlet-A	65 -> 81	0.67901
35	7.114	0.0367	Singlet-A	54 -> 66	0.58330
36	7.196	0.0054	Singlet-A	65 -> 83	0.67919
37	7.221	0.0047	Singlet-A	65 -> 82	0.64654
38	7.240	0.1074	Singlet-A	63 -> 71	0.58712
39	7.260	0.0295	Singlet-A	64 -> 73	0.44786
40	7.272	0.0002	Singlet-A	53 -> 66	0.66763

Table S14. TD-DFT calculated vertical exitation energies (E_{exc}), oscilator strenght (f) and leading configurations for **14** at the PBE0/6-311+G(2d,p)//PBE0/6-311G(2d,p) level of theory.

Root	E_{exc}/eV	f	Leading configuration		Weight
1	4.974	0.0569	Singlet-A	41 -> 42	0.64911
2	5.473	0.0046	Singlet-A	41 -> 43	0.66461
3	5.713	0.0242	Singlet-A	41 -> 44	0.56236
4	5.835	0.0024	Singlet-A	41 -> 45	0.54162

5	5.863	0.0102	Singlet-A	39 -> 42	0.46028
6	6.085	0.0001	Singlet-A	41 -> 46	0.64360
7	6.125	0.0104	Singlet-A	40 -> 43	0.56163
8	6.244	0.0163	Singlet-A	41 -> 47	0.61120
9	6.338	0.0134	Singlet-A	40 -> 44	0.54599
10	6.386	0.0568	Singlet-A	39 -> 43	0.47327
11	6.423	0.0016	Singlet-A	41 -> 48	0.63522
12	6.547	0.2436	Singlet-A	39 -> 42	0.38703
13	6.595	0.0360	Singlet-A	41 -> 49	0.63792
14	6.640	0.1884	Singlet-A	39 -> 44	0.36972
15	6.752	0.0762	Singlet-A	41 -> 50	0.48137
16	6.789	0.1013	Singlet-A	39 -> 45	0.50501
17	6.820	0.2258	Singlet-A	41 -> 50	0.43239
18	6.911	0.0077	Singlet-A	40 -> 47	0.39997
19	6.935	0.0318	Singlet-A	41 -> 51	0.64979
20	6.969	0.0375	Singlet-A	40 -> 46	0.37604
21	7.020	0.0626	Singlet-A	39 -> 46	0.46007
22	7.025	0.0564	Singlet-A	41 -> 52	0.58765
23	7.198	0.0054	Singlet-A	41 -> 53	0.65033
24	7.240	0.0393	Singlet-A	39 -> 47	0.48834
25	7.251	0.0025	Singlet-A	41 -> 54	0.53936
26	7.262	0.0037	Singlet-A	40 -> 48	0.41998
27	7.345	0.0050	Singlet-A	39 -> 48	0.46279
28	7.381	0.0006	Singlet-A	41 -> 55	0.58132
29	7.400	0.0104	Singlet-A	40 -> 49	0.36367
30	7.489	0.0016	Singlet-A	40 -> 49	0.48805
31	7.588	0.0219	Singlet-A	41 -> 56	0.66379
32	7.611	0.0182	Singlet-A	39 -> 49	0.46647
33	7.640	0.0277	Singlet-A	38 -> 42	0.58302
34	7.698	0.0038	Singlet-A	39 -> 50	0.49447
35	7.722	0.0052	Singlet-A	40 -> 52	0.42361
36	7.830	0.0049	Singlet-A	40 -> 51	0.40084
37	7.867	0.0130	Singlet-A	39 -> 51	0.46858
38	7.929	0.0123	Singlet-A	39 -> 52	0.53974
39	7.970	0.0001	Singlet-A	41 -> 57	0.51101
40	8.008	0.0046	Singlet-A	38 -> 44	0.45397

Table S15. Cartesian geometries (Å) for stationary points in the ground (S_0) and the first excited singlet state (S_1) calculated at the PBE0/6-311G(2d,p) level of theory

3 (S_0)

B	3.577638	0.214106	0.317566
N	2.557591	1.345077	0.044437
C	1.209985	1.172992	-0.242695
C	0.655486	-0.106711	-0.305645
C	1.441266	-1.238790	-0.085804
N	2.794826	-1.115271	0.199949
C	2.837265	2.652135	0.034720
C	0.636626	2.462870	-0.441053
C	-0.786858	-0.266537	-0.612916
C	1.118523	-2.627864	-0.085933
C	3.312220	-2.335615	0.371018
C	2.298222	-3.290382	0.199707
C	1.667529	3.367495	-0.262323
F	4.594608	0.252578	-0.623837
F	4.104015	0.345820	1.593777
C	4.196227	3.182640	0.300734
H	1.598313	4.443281	-0.339243
C	-0.768024	2.832607	-0.774194
C	4.742169	-2.562632	0.691897
H	2.430048	-4.359966	0.281068
C	-0.190978	-3.294581	-0.332438
C	-1.220994	-0.457785	-1.921646
C	-2.567071	-0.595827	-2.207863
C	-3.511916	-0.562685	-1.185060
C	-3.090011	-0.389830	0.143455
C	-1.735861	-0.229849	0.402061
H	-0.493509	-0.486935	-2.726321
H	-2.914680	-0.730667	-3.225794
O	-4.810910	-0.699336	-1.496729
C	-4.091969	-0.455652	1.263846
H	-1.408576	-0.085388	1.428365
H	-3.643040	-0.072822	2.195203
N	-5.340311	0.239934	0.949390
H	-4.354561	-1.504874	1.446586
C	-6.386670	-0.101706	1.894846
C	-5.150236	1.679076	0.873818
H	-7.316600	0.392754	1.607540
H	-6.555240	-1.180507	1.888485
H	-6.135555	0.206040	2.922811
H	-6.078874	2.154787	0.552860
H	-4.855823	2.105956	1.846096
H	-4.373079	1.912509	0.144176
H	-5.316382	-0.419328	-0.690872
H	-0.837225	3.910659	-0.931262
H	-1.123015	2.330287	-1.676430
H	-1.460155	2.561499	0.027336
H	-0.086018	-4.372757	-0.198393
H	-0.966886	-2.937805	0.348530
H	-0.559004	-3.111987	-1.344760
H	4.195005	4.271598	0.258444
H	4.548188	2.858482	1.283078
H	4.907548	2.793069	-0.431630
H	4.945881	-3.628856	0.788150
H	5.380766	-2.141367	-0.088340

H	5.009629	-2.057486	1.623239

13 (S_0)

B	-0.000003	1.229079	0.026176
N	-1.244614	0.282599	-0.019767
C	-1.208733	-1.099029	0.015753
C	0.000003	-1.772083	0.037053
C	1.208741	-1.099029	0.015836
N	1.244610	0.282598	-0.019793
C	-2.520132	0.656227	-0.056953
C	-2.537312	-1.576475	-0.000225
H	0.000005	-2.855943	0.061352
C	2.537322	-1.576468	-0.000152
C	2.520124	0.656231	-0.057015
C	3.360684	-0.470247	-0.046973
C	-3.360682	-0.470257	-0.046968
F	-0.000005	2.059676	-1.067082
F	0.000000	1.939299	1.202041
H	-2.786267	1.703033	-0.089051
H	-4.439140	-0.451086	-0.073517
H	-2.827223	-2.616870	0.016615
H	2.786247	1.703035	-0.089273
H	4.439141	-0.451075	-0.073535
H	2.827240	-2.616861	0.016683

12 (S_0)

B	-0.000104	-1.331223	-0.000364
N	1.246556	-0.399339	-0.000730
C	1.208146	0.985424	0.002754
C	0.000043	1.656485	0.006106
C	-1.208098	0.985376	0.002827
N	-1.246572	-0.399342	-0.000780
C	2.527826	-0.782657	-0.000638
C	2.538112	1.475606	0.003904
H	-0.000029	2.740896	0.011160
C	-2.537962	1.475672	0.003966
C	-2.527954	-0.782588	-0.000748
C	-3.352664	0.358888	0.002152
C	3.352690	0.358800	0.002235
F	0.000024	-2.121108	-1.136680
F	-0.000027	-2.120840	1.136165
C	2.932950	-2.208562	-0.001545
H	4.433219	0.342702	0.003729
C	2.950995	2.905721	-0.004736
C	-2.933049	-2.208497	-0.001833
H	-4.433197	0.342981	0.003710
C	-2.950904	2.905786	-0.004391
H	2.689086	3.392450	-0.949337
H	2.468961	3.470913	0.797844
H	4.030118	2.997045	0.125717
H	-2.469607	3.470648	0.798873
H	-4.030146	2.996940	0.125156
H	-2.688194	3.392982	-0.948524
H	4.018861	-2.298526	-0.002400
H	2.528285	-2.720140	0.875374
H	2.526942	-2.719360	-0.878275
H	-4.018962	-2.298484	-0.002649
H	-2.527096	-2.719160	-0.878663
H	-2.528360	-2.720201	0.875002

14 (S_0)

H	3.391387	-1.974364	0.156320
C	2.669385	-1.171077	0.066292
C	3.065634	0.152806	0.200030
C	2.140325	1.177208	0.099075
C	0.801809	0.889370	-0.151623
C	0.391187	-0.443777	-0.309628
C	1.335458	-1.454302	-0.183508
H	4.105905	0.391332	0.395432
H	2.429346	2.215749	0.214661
O	-0.075939	1.907158	-0.240065
C	-1.032730	-0.747842	-0.684315
H	1.013507	-2.486279	-0.295039
H	-1.231685	-1.826267	-0.565675
N	-2.001111	0.055793	0.063550
H	-1.183974	-0.512456	-1.745107
C	-3.326416	-0.041777	-0.516084
C	-2.017455	-0.297087	1.472902
H	-4.016217	0.603963	0.031153
H	-3.301602	0.286229	-1.557422
H	-3.720095	-1.071289	-0.484755
H	-2.676023	0.384916	2.014457
H	-2.372692	-1.328240	1.633763
H	-1.011989	-0.211005	1.887576
H	-0.973763	1.498759	-0.168542

5. Biological investigation

Cell culture

Human lung carcinoma cells H460, colon carcinoma HCT116 and breast cancer cells MCF-7 were grown in DMEM medium with the addition of 10% fetal bovine serum (FBS), 2 mM L-glutamine, 100 U/mL penicillin and 100 μg/mL streptomycin, and cultured as monolayers at 37°C in a humidified atmosphere with 5% CO_2.

Cell viability assay

Cell viability assay was performed as described previously.[18] The cells were inoculated in parallel on three 96-well microtiter plates on day 0, at 3×10^4 cells/mL (H460, HCT116), 4.5×10^4 cells/mL (MCF-7). Test agents were added in ten-fold dilutions (10^{-8} to 10^{-4} M) on the next day and incubated for further 72 h. Working dilutions were freshly prepared on the day of testing. One of the plates was left in the dark, while the other two plates were irradiated in a Luzchem reactor (6 lamps 300 nm, 1 min) at 4, 28, and 52 h after the addition of the tested compounds. After 72 h of incubation the cell growth rate was evaluated by performing the MTT assay. The absorbance (*A*) was measured on a microplate reader at 570 nm. The absorbance is directly proportional to the number of living, metabolically active cells. The IC_{50} values are calculated from concentration-response curve using linear regression analysis. Each test was performed in quadruplicate in at least two individual experiments.

Table S16. IC_{50} values obtained by MTT test on three human cancer cell lines.

	MCF-7		**H460**		**HCT 116**	
	Not irrad.	**300nm, 3×1 min**	**Not irrad.**	**300nm, 3×1 min**	**Not irrad.**	**300nm, 3×1 min**
2	11±0.4	14±6	≥100	≥100	17±8	20±3
4	3±2	2±1	14±2	13±1	10±0.1	8±1

Confocal microscopy

Live cell confocal fluorescence microscopy was performed to assess the intracellular distribution of compounds. Briefly, MCF-7 cells were seeded on cell culture imaging dishes (ibiTreat, 35 mm, Ibidi, Germany) (70 000 cells/dish) and grown at 37°C for 24 h, as described above. The cells were then incubated with compound **4** (c = 10 μM) for 1 h. Dishes were rinsed twice with PBS, and immediately analyzed. The uptake and intracellular distribution of tested dyes were analyzed under Leica TCS SP8 X confocal microscope (Leica Microsystems, Germany) with excitation wavelength 490 nm, and emission detection at 510-540 nm.

Selected images:

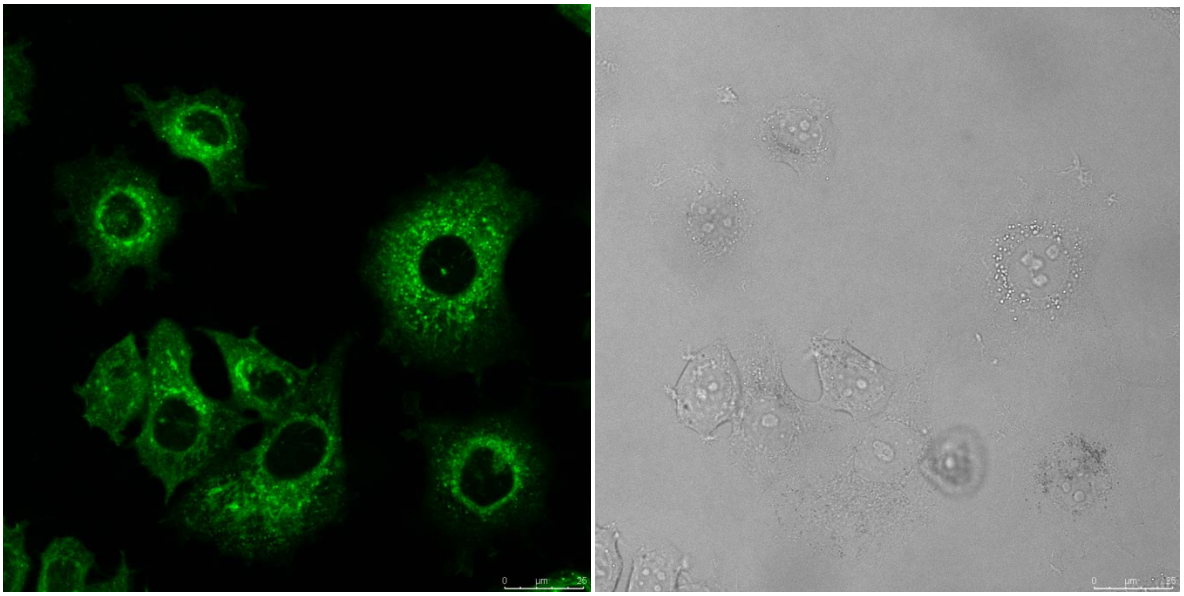

Figure S31. Confocal microscopy images of MCF-7 cells. Left panel - the fluorescence images, excitation at λ_{ex} = 490 nm and detection at 510-540 nm; right panel – the same image in the transmitted light. The cells were treated with compound **4** (c = 10 μM) for 1 h, rinsed and analyzed by confocal microscopy.

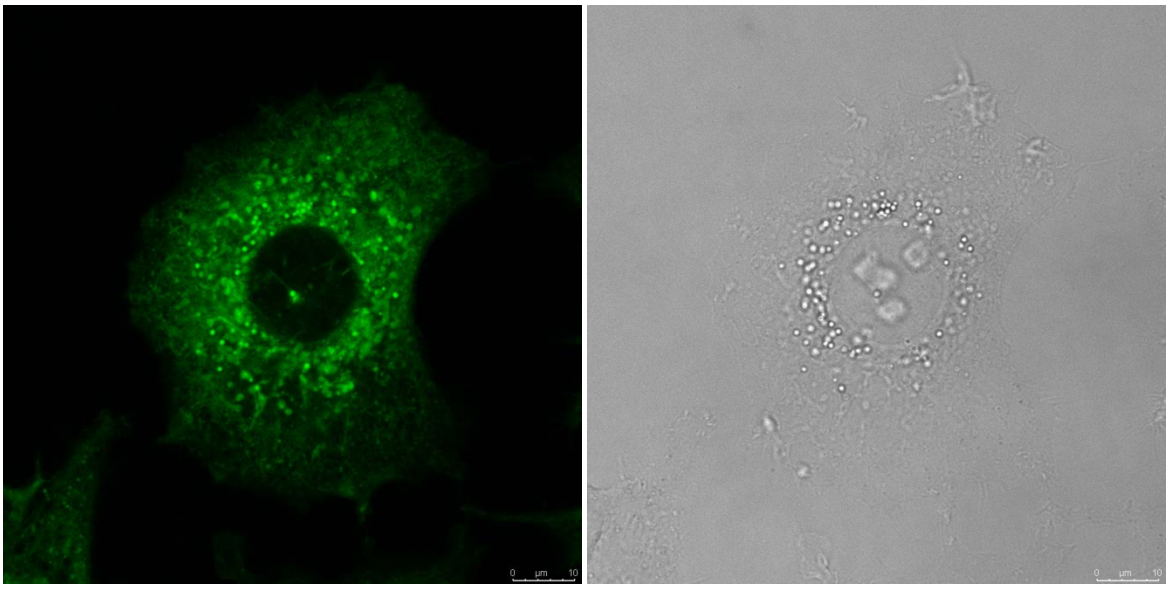

Figure S32. Confocal microscopy images of MCF-7 cells. Left panel - the fluorescence images, excitation at λ_{ex} = 490 nm and detection at 510-540 nm; right panel – the same image in the transmitted light. The cells were treated with compound **4** (c = 10 μM) for 1 h, rinsed and analyzed by confocal microscopy.

Non-covalent binding to proteins

Fluorescence titrations for **2** and **4** with bovine serum albumin (BSA) were conducted to assay noncovalent binding. The measurements were performed on an Agilent Cary Eclipse fluorometer by use of slits corresponding to the bandpass of 5 nm for the excitation and 5.0 nm for the emission. Solution of **2** (c = 2.6 × 10^{-6} M) and **4** (c = 3.2 × 10^{-5} M) were prepared in CH_3CN - H_2O (1:4) in the presence of sodium phosphate buffer (c = 0.05 M, pH = 7.0). A stock solution of BSA (bovine serum albumin, Sigma) in the phosphate buffer was prepared by dissolving (33.3 mg of the protein in 1 mL buffer (c = 5.0 × 10^{-4} M). A fluorescence cell was filled with the solution of **2** or **4** (2 mL) and titrated with the solution of BSA (50 μL additions). After each addition, the solution was left to equilibrate for 5-15 min, and the fluorescence spectra were recorded by exciting at 460 nm, whereas fluorescence was recorded in the range 470-800 nm. The titration was performed at 25 °C.

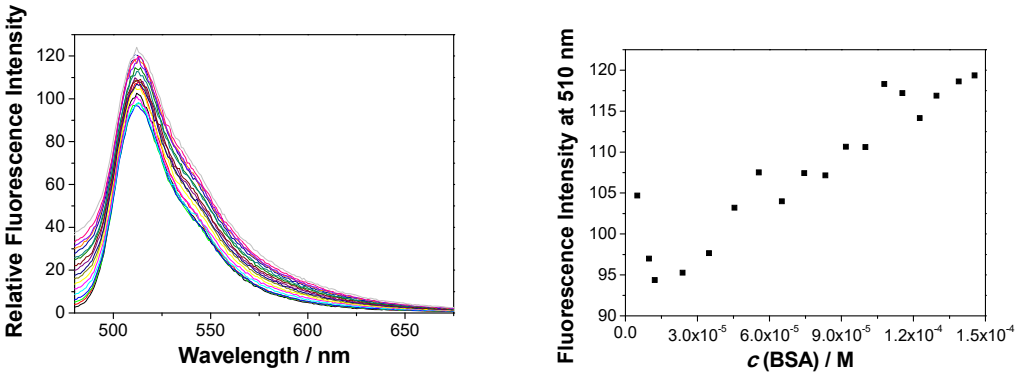

Figure S33. Fluorescence spectra (λ_{ex} = 460 nm) of **2** in CH_3CN-H_2O (1:4, phosphate buffer pH = 7.0, c = 0.05 M), with increasing concentration of BSA (left); Dependence of the fluorescence intensity at 510 nm on the BSA concentration (right).

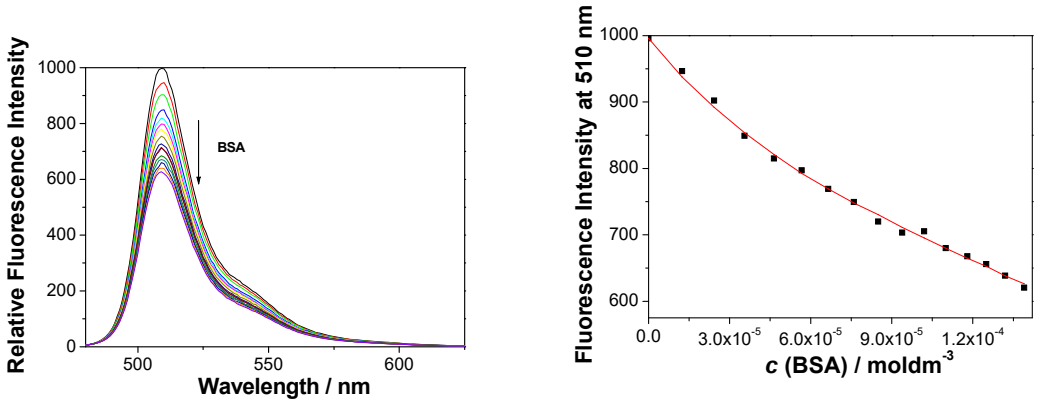

Figure S34. Fluorescence spectra (λ_{ex} = 460 nm) of **4** in CH_3CN-H_2O (1:4, phosphate buffer pH = 7.0, c = 0.05 M), with increasing concentration of BSA (left); Dependence of the fluorescence intensity at 510 nm on the BSA concentration (right). The fluorescence data was processed by multivariate non-linear regression analysis using model for the formation of a complex **1@BSA** 1:1, logβ = 4.70 ± 0.08. Dots are the experimental value, whereas the red line represent the fitted value.

Fluorescence staining of protein

Samples containing 20 µg of bovine serum albumin BSA (Albumin standard, Thermo scientific, USA) were incubated without **4**, or with **4** (c =1 mM, or c = 0.1 mM), and irradiated in a Luzchem reactor (6 lamps at 350 nm) for 30 min. After photoinduced labelling of BSA, the samples were run on a SDS-PAGE gel (10%). The labeled BSA was visualized in the gel using a UV light at 254 nm (Figure 3 in the manuscript). Alternatively, the labeled BSA was visualized in the gel using a light at 254 nm (Image Master VDS, Pharmacia Biotech, Sweden,

Figure S35 bottom panel). Subsequently the same gel was stained with Coomassie brilliant blue (Figure S35 top panel).

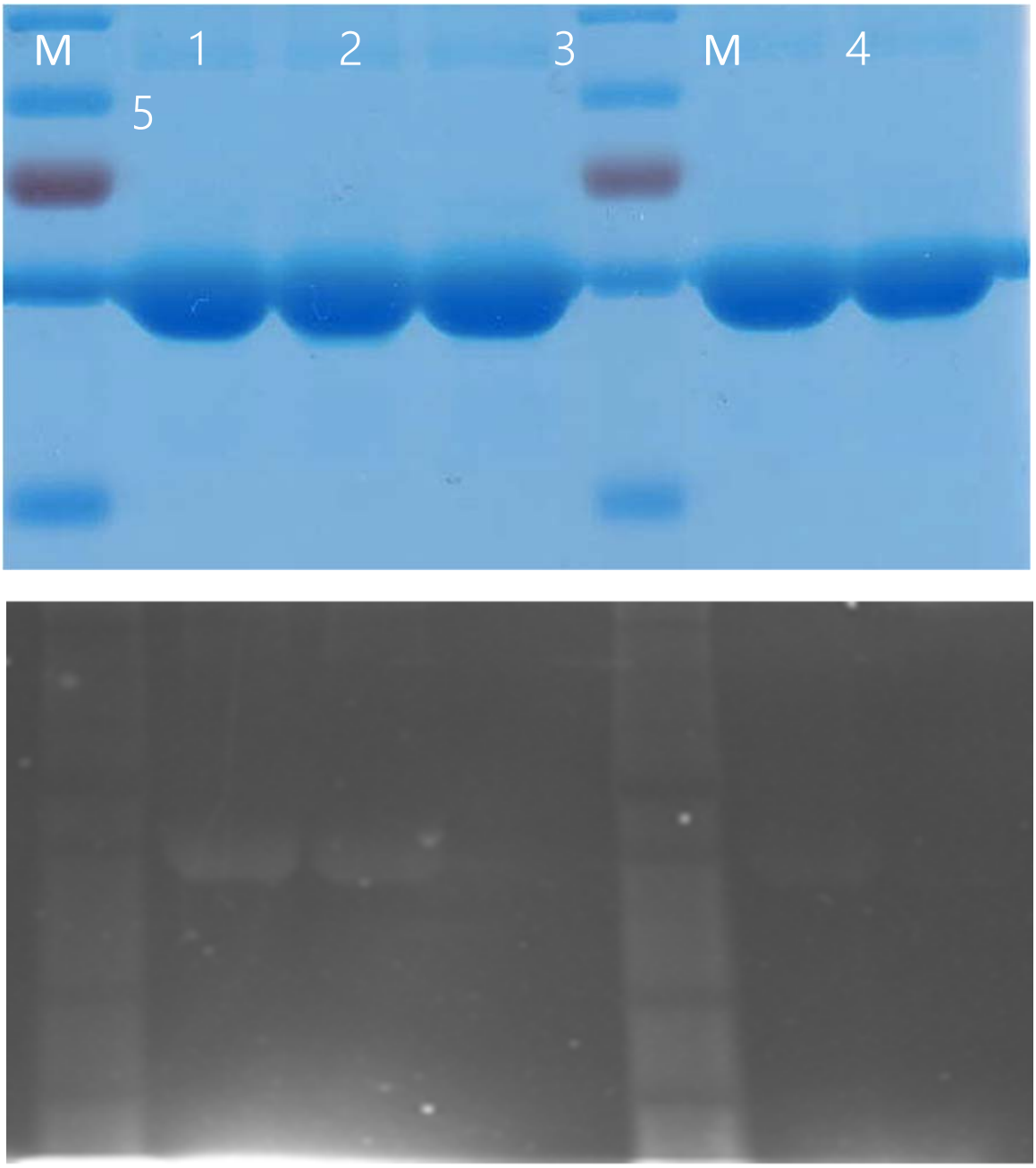

Figure S35. SDS-PAGE gel (10%) after photoinduced labelling of BSA with **4.** The BSA (20 µg) was incubated with or without **4**, irradiated at 350 nm (30 min, 6 lamps) or not irradiated, and then subjected to SDS-PAGE: Lane 1 with **4** (c = 0.1 mM); irradiated at 350 nm for 30 min; Lanes 2 with **4** (c = 1 mM); irradiated at 350 nm for 30 min; Lane 3 without **4**; irradiated at 350 nm for 30 min; Lane 4 with **4** (c = 1 mM), not irradiated; Lane 5 without **4**; not irradiated; Lane M - Precision Plus Protein™ Standard. The labeled BSA was visualized in the gel using a light at 254 nm (Image Master VDS, Pharmacia Biotech, Sweden, bottom panel). Subsequently the same gel was stained with Coomassie brilliant blue (Figure S35 top panel).

Photoinduced covalent modification of proteins

A solution of **2** ($c = 2.6 \times 10^{-6}$ M) or **4** ($c = 3.2 \times 10^{-5}$ M) in CH_3CN - H_2O (1:4) in the presence of sodium phosphate buffer (c = 0.05 M, pH = 7.0) and BSA ($c = 1.4 \times 10^{-4}$ M) were irradiated in the fluorescence cells (2.5 mL in a cell) in a Luzchem reactor at 350 nm (8 lamps, 1 lamp 8 W) for 1 h. After the irradiation, the samples for the MS analysis were prepared as we described previously,[19] and they were analyzed by MALDI-TOF/TOF MS spectrometry.

Table S17. Molecular weight (Da) of BSA before and after the irradiation (λ = 350 nm) in the presence of **2** or **4**.

Exp.	BSA $^{2+}$	BSA $^{+}$	BSA + **2** $^{2+}$	BSA + **2** $^{+}$	BSA + **4** $^{2+}$	BSA + **4** $^{+}$
1	33240	66479	33605.2	67209.4	33658.8	67316.6
2	33248.7	66496.4	33621.3	67241.6	33661.4	67321.8
3	33245.8	66490.6	33632.4	67263.8	33654.7	67308.4
4	33245.7	66490.4	33401.1	66801.2	33643.5	67286
5	33252.5	66504	33618.1	67235.2	33648.2	67295.4
6	33233.8	66466.6	33608.9	67216.8	33680.2	67359.4
7	33218.9	66436.8	33630.7	67260.4	33670.7	67340.4
8	33239.6	66478.2	33619.6	67238.2	33649.8	67298.6
9	33256.6	66512.2	33622.1	67243.2	33647.7	67294.4
10	33262.8	66524.6	33631.3	67261.6	33655.3	67309.6
Average	**33244.44**	**66487.88**	**33599.07**	**67197.14**	**33657.03**	**67313.06**

6. NMR spectra

^{1}H NMR (CD_3OD, 300 MHz):

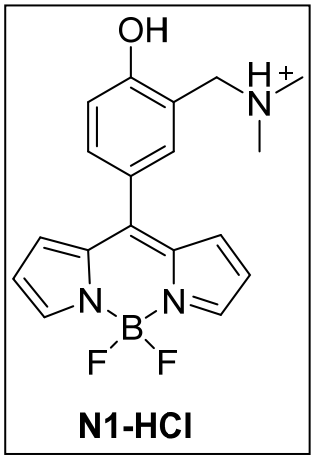

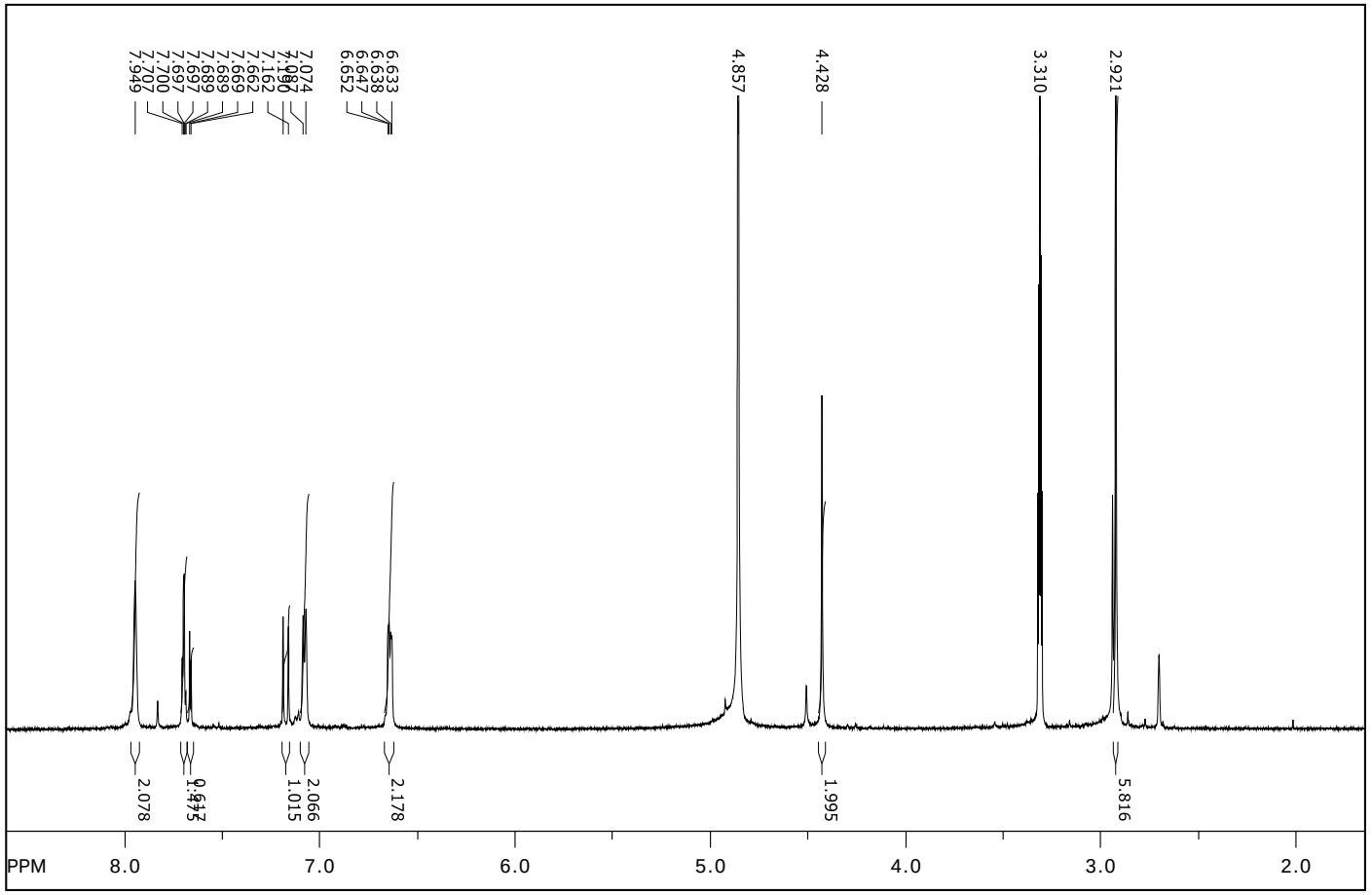

^{13}C NMR (CD_3OD, 75 MHz, APT):

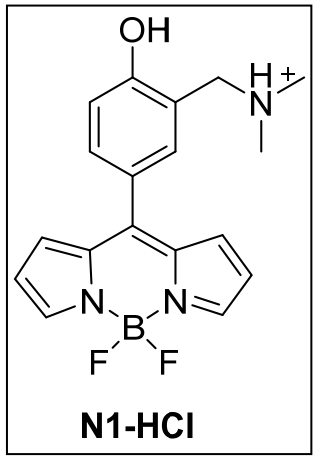

N1-HCl

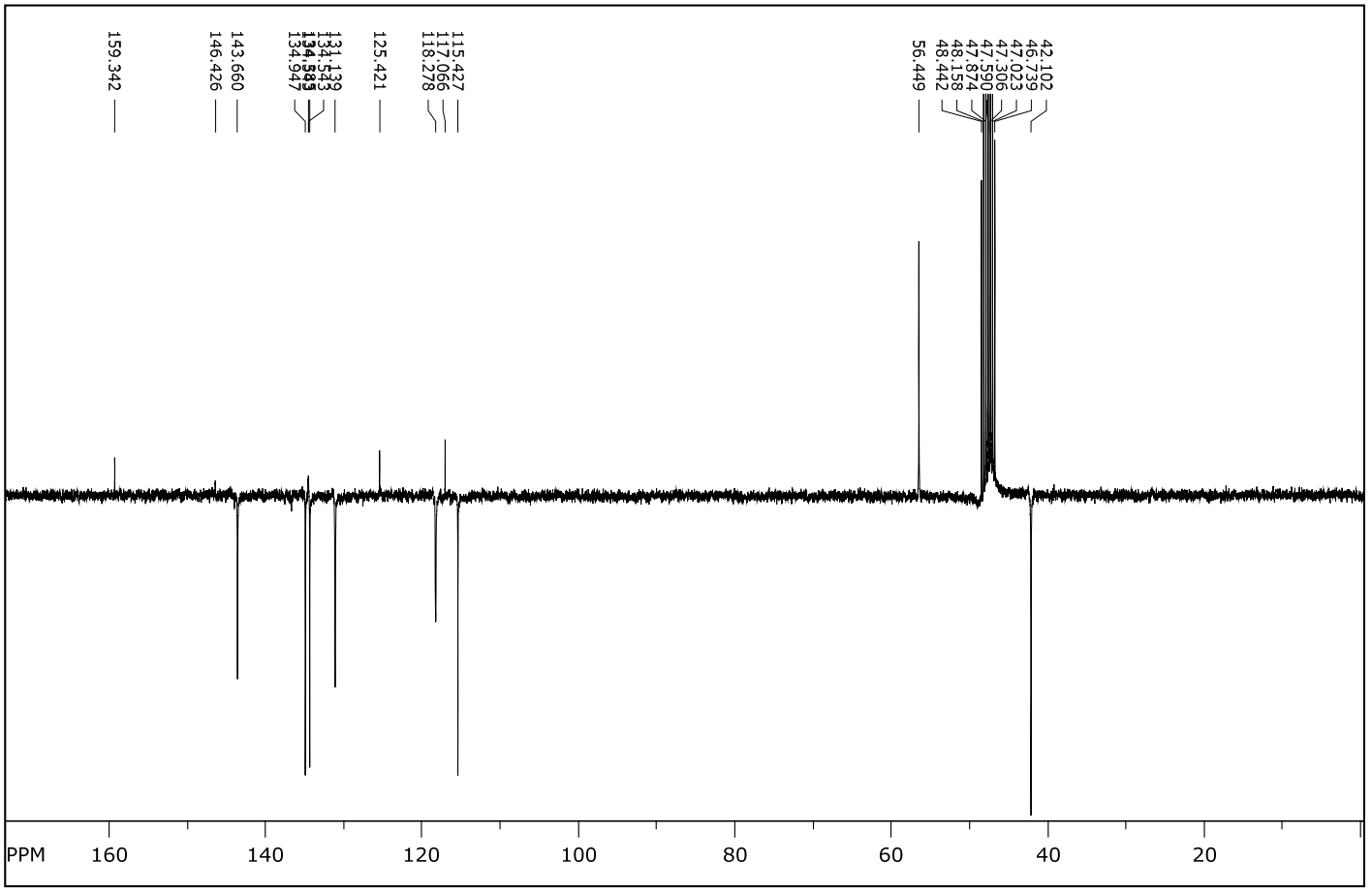

^{1}H NMR (CD_3OD, 300 MHz):

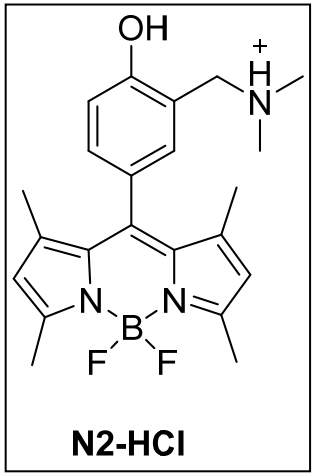

N2-HCl

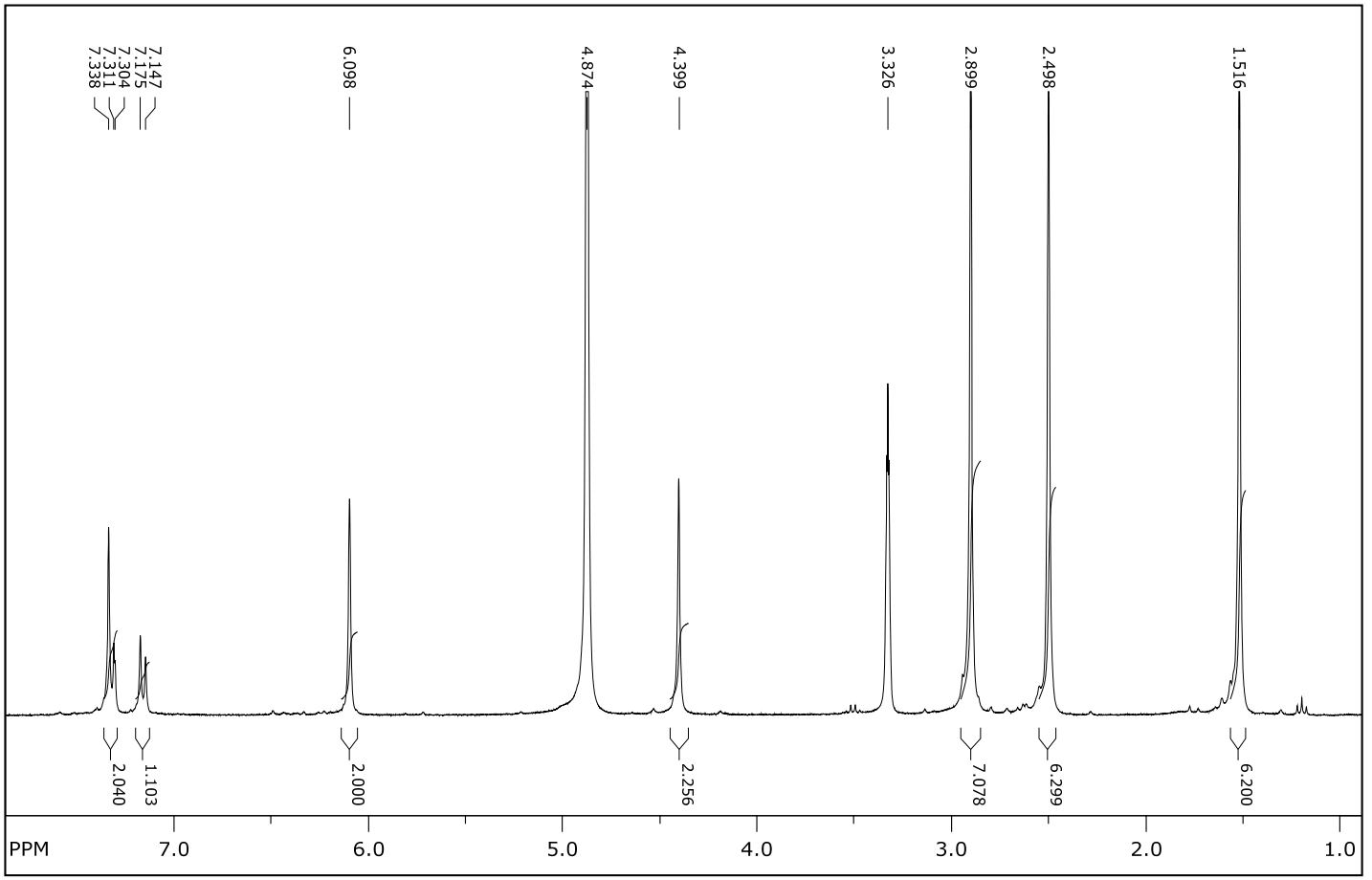

^{13}C NMR (CD_3OD, 75 MHz):

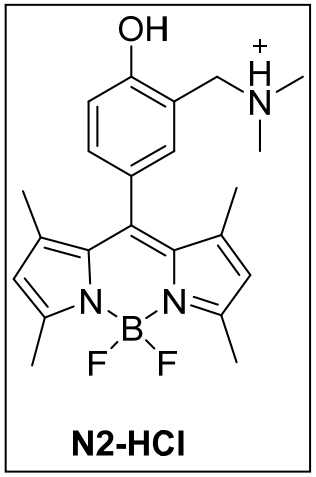

N2-HCl

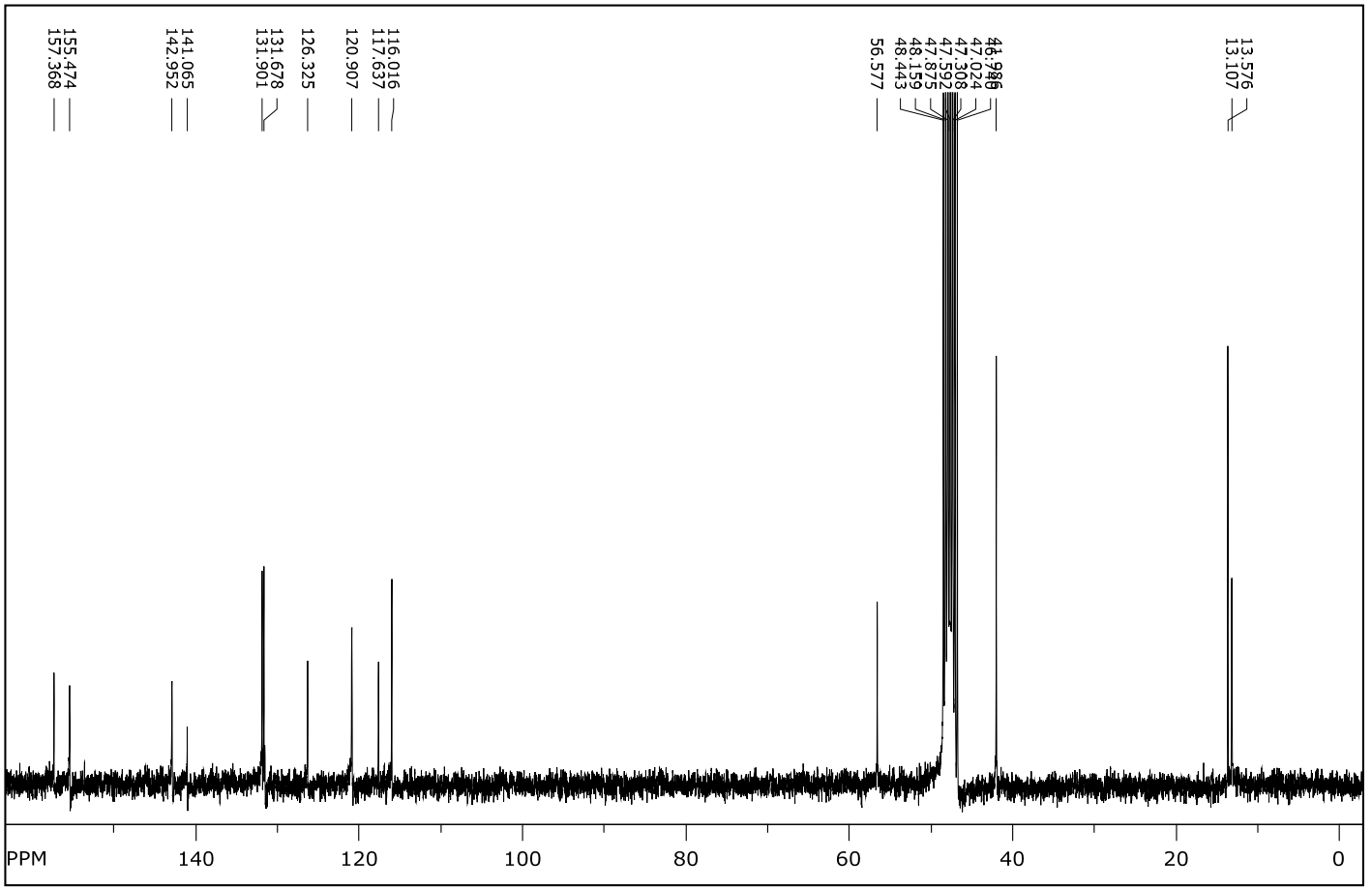

^{13}C NMR (CD_3OD, 75 MHz, APT):

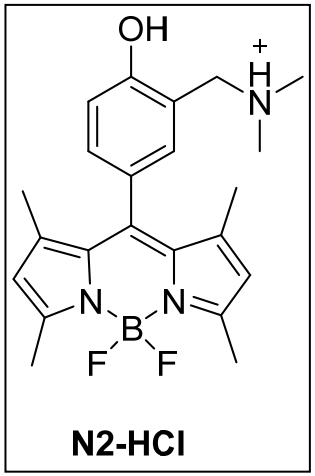

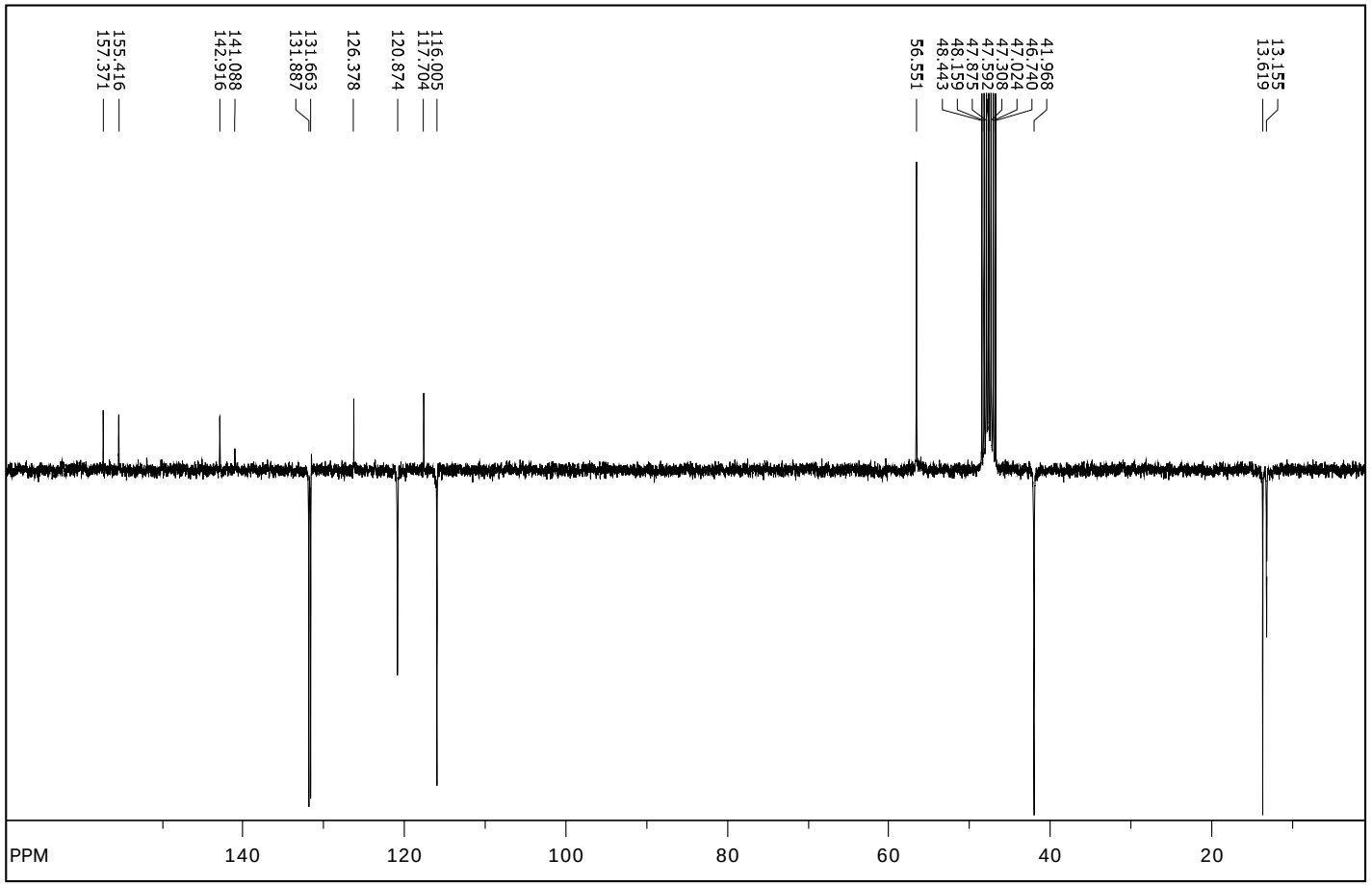

^{1}H NMR (CD_3OD, 300 MHz):

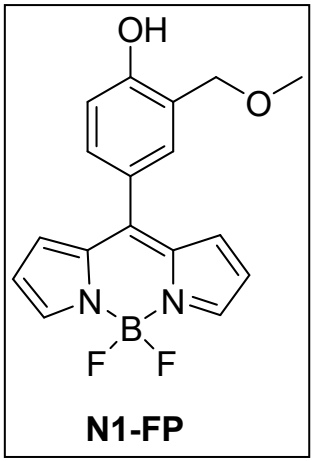

N1-FP

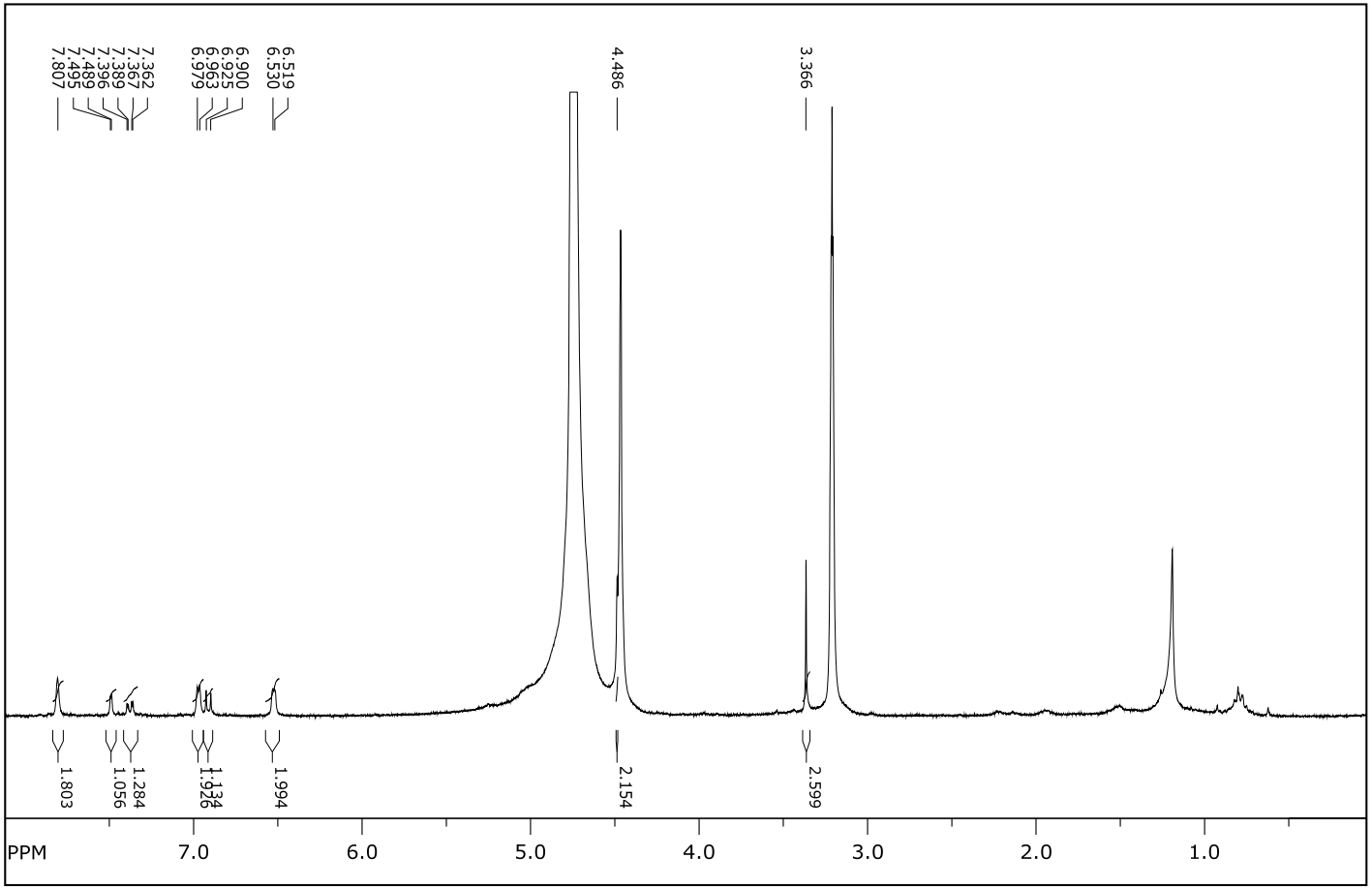

^{13}C NMR (CD_3OD, 75 MHz):

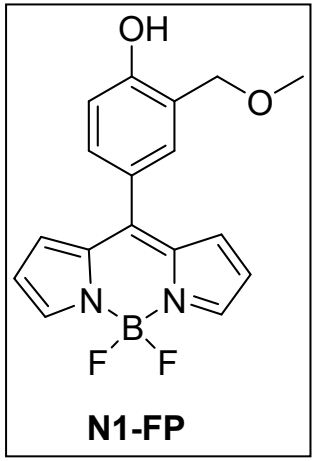

N1-FP

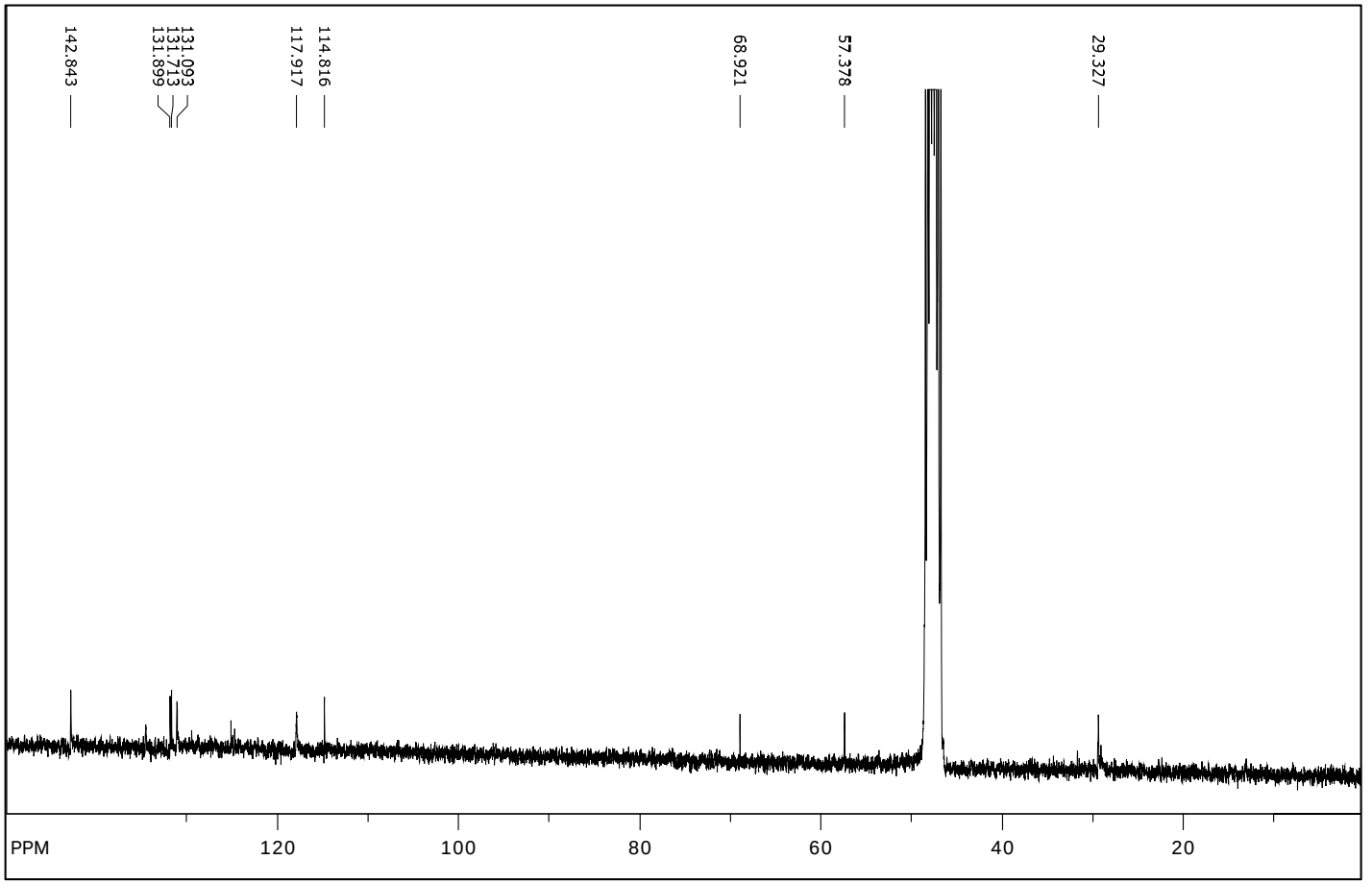

^{1}H NMR (CD_3OD, 300 MHz):

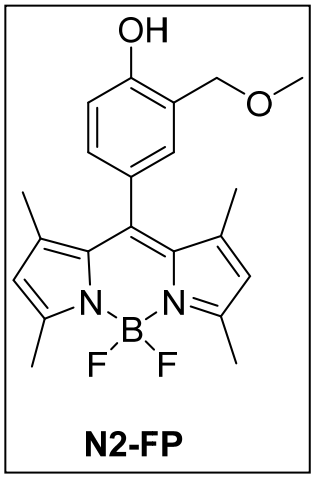

N2-FP

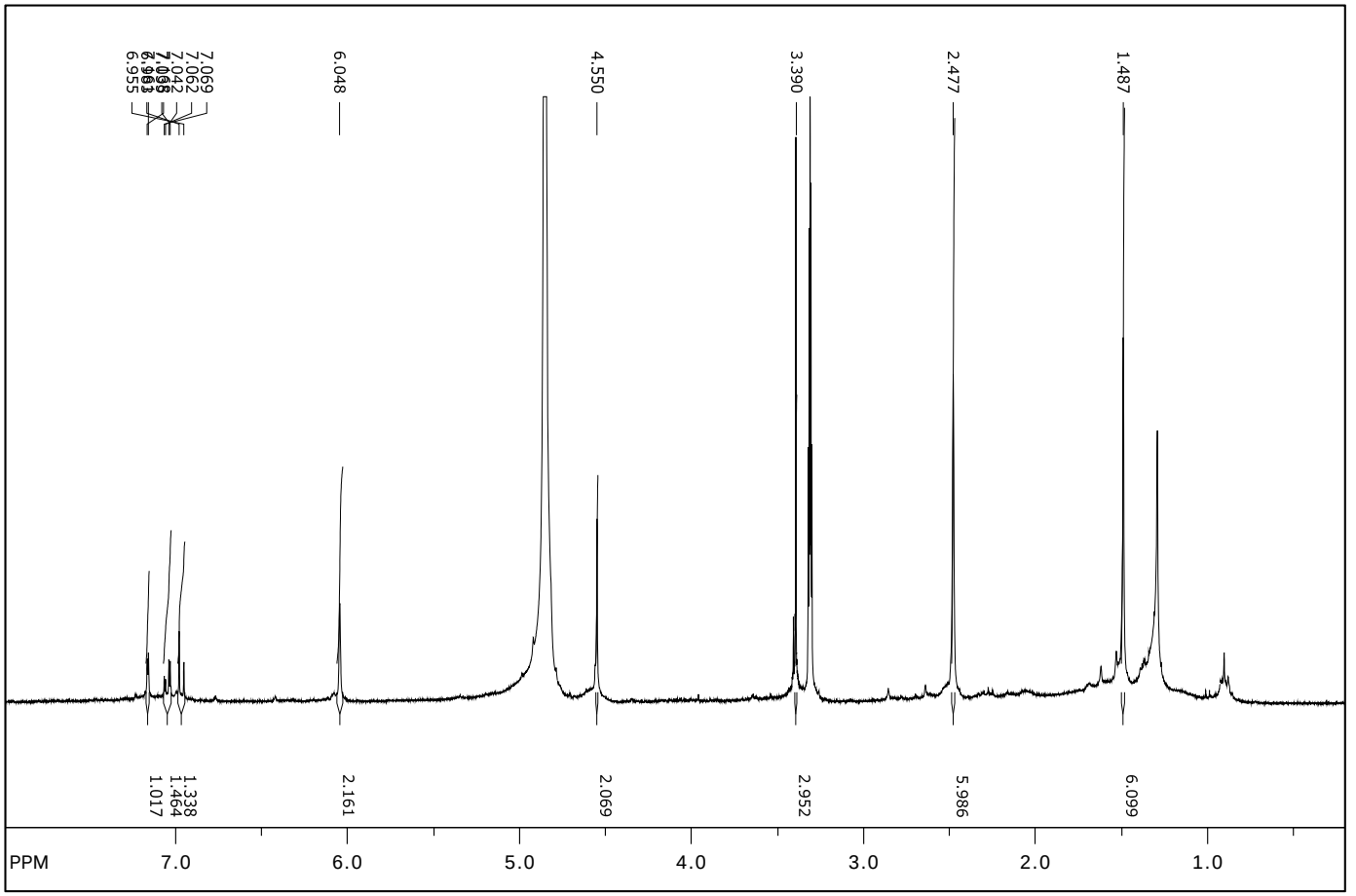

^{13}C NMR (CD_3OD, 75 MHz, APT):

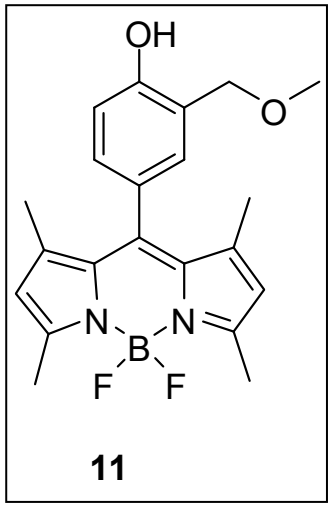

11

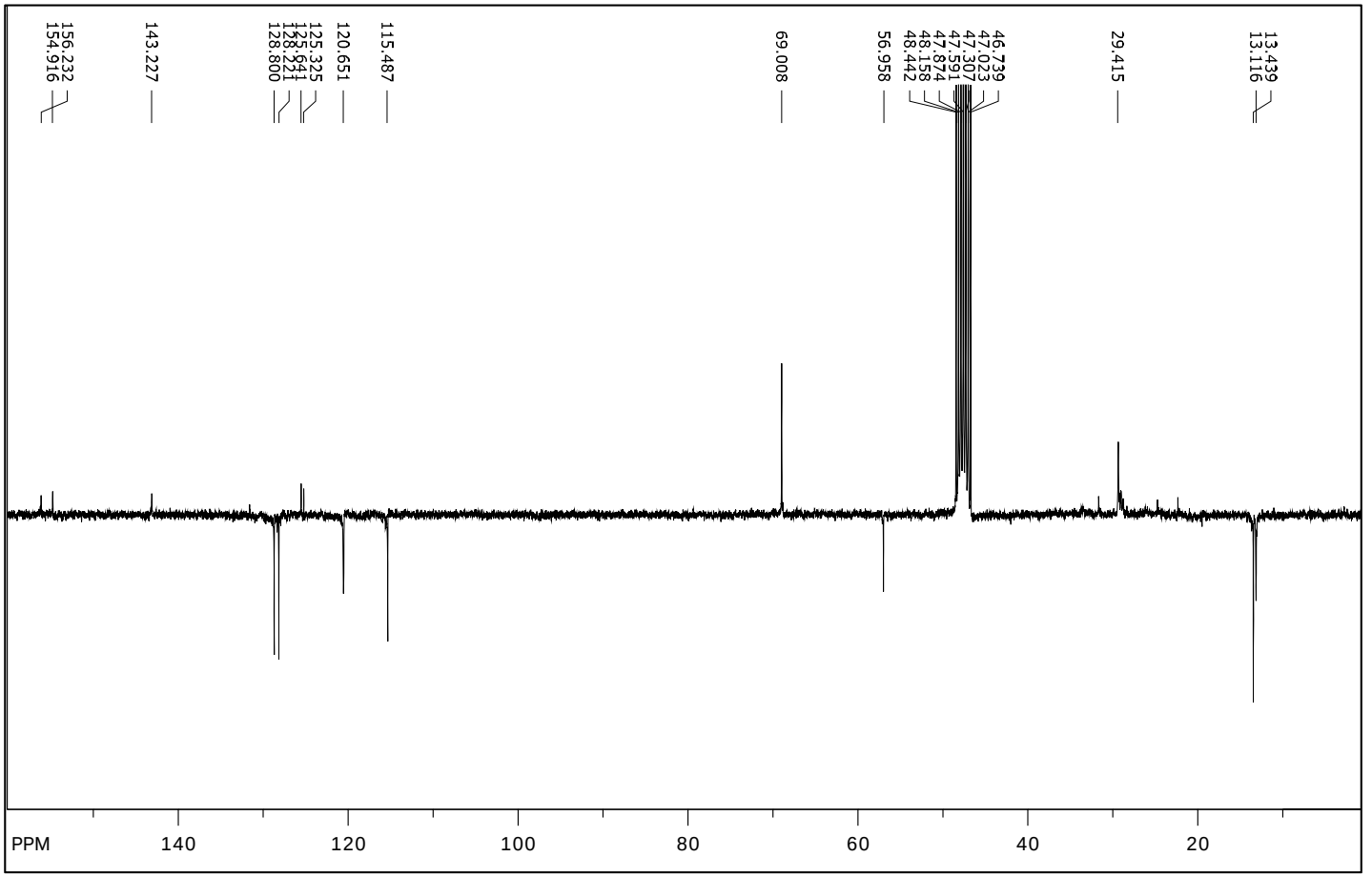

7. References

[1] Baruah, M.; Qin, W.; Basarić, N.; De Broggraeve, W. M.; Boens, N., BODIPY-Based Hydroxyaryl Derivatives as Fluorescent pH Probes, *J. Org. Chem*. **2005**, *70*, 4152-4157.

[2] Yan, Z.; Lin, X.; Guo, H.; Yang, F., A Novel Fluorescence Sensor for K^+ Based on Bis-BODIPY: The ACQ effect Controlled by Cation Complexation of Pseudo Crown Ether Ring, *Tetrahedron Lett.* 2017, 58, 3064-3068.

[3] Coskun, A.; Deniz, E.; Akkaya, E. U., Effective PET and ICT Switching of Boradiazaindacene Emission: A Unimolecular, Emission-Mode, Molecular Half-Subtractor with Reconfigurable Logic Gates, *Org. Lett*. **2005**, *7*, 5187-5189.

[4] Montalti, M.; Credi, A.; Prodi, L.; Gandolfi, M. T., in *Handbook of Photochemistry*; CRC Taylor and Francis: Boca Raton, 2006; Goldstein, S.; Rabani, J., The Ferrioxalate and Iodide-Iodate Actinometers in the UV Region, *J. Photochem. Photobiol*. **2008**, *193*, 50-55.

[5] Olmsted, J. III, Calorimetric Determinations of Absolute Fluorescence Quantum Yields, *J. Phys. Chem*. **1979**, *83*, 2581-2584.

[6] Liao, Y.; Bohne, C., Alcohol Effect on Equilibrium Constants and Dissociation Dynamics of Xanthone-Cyclodextrin Complexes. *J. Phys. Chem.,* **1996**, *100,* 734-743.

[7] Mitchell, R. H.; Bohne, C.; Wang, Y.; Bandyopadhyay, S.; Wozniak, C. B., Multistate π Switches: Synthesis and Photochemistry of a Molecule Containing Three Switchable Annelated Dihydropyrene Units, *J. Org. Chem*. **2006**, *71*, 327-336.

[8] Runge, E.; Gross, E. K. U., Density-Functional Theory for Time-Dependent Systems, *Phys. Rev. Lett*. **1984**, *52*, 997-1000.

[9] Adamo, C.; Barone, V., Toward Reliable Density Functional Methods without Adjustable Parameters: The PBE0 Model, *J. Chem. Phys*. **1999**, *110*, 6158-6170.

[10] Boese, A. D.; Martin, J. M. L., Development of Density Functionals for Thermochemical Kinetics. *J. Chem. Phys*. **2004**, *121*, 3405-3416.

[11] Yanai, T.; Tew, D. P.; Handy, N. C., A New Hybrid Exchange–Correlation Functional Using the Coulomb-Attenuating Method (CAM-B3LYP), *Chem. Phys. Lett*. **2004**, *393*, 51-57.

[12] Zhao, Y.; Truhlar, D. G.; The M06 Suite of Density Functionals for Main Group Thermochemistry, Thermochemical Kinetics, Noncovalent Interactions, Excited States, and Transition Elements: Two New Functionals and Systematic Testing of Four M06-Class Functionals and 12 Other Functionals, *Theor. Chem. Acc*. **2008**, *120*, 215-241.

[13] Laurent, D.; Jacquemin, D., TD-DFT Benchmarks: A Review. *Int. J. Quantum Chem*. **2013**, *113*, 2019-2039 and references therein.

[14] Antol, I.; Glasovac, Z.; Margetić, D.; Crespo-Otero, R.; Barbatti, M., Insights on the Auxochromic Properties of the Guanidinium Group, *J. Phys. Chem. A* **2016**, *120*, 7088-7100.

[15] Frisch, M. J.; Trucks, G. W.; Schlegel, H. B.; Scuseria, G. E.; Robb, M. A.; Cheeseman, J. R.; Scalmani, G.; Barone, V.; Mennucci, B.; Petersson, G. A., *et al*, Gaussian 09, revision D.01; Gaussian, Inc.: Wallingford, CT, 2009.

[16] Pedretti, A.; Villa, L.; Vistoli, G.; VEGA: a Versatile Program to Convert, Handle and Visualize Molecular Structure on Windows-based PCs, *J. Mol. Graph*. **2002**, *21*, 47-49.

[17] Schaftenaar, G.; Noordik, J. H., Molden: a Pre- and Post-Processing Program for Molecular and Electronic Structures. *J. Comp. Aided Mol. Design* **2000**, *14*, 123-134.

[18] Uzelac, L.; Škalamera, Đ.; Mlinarić-Majerski, K.; Basarić, N.; Kralj, M., Selective Photocytotoxicity of Anthrols on Cancer Stem-like Cells: The Effect of Quinone Methides or Reactive Oxygen Species, *Eur. J. Med. Chem*. **2017**,*137*, 558-574.

[19] Sambol, M.; Ester, K.; Landgraf, S.; Mihaljević, B.; Cindrić, M.; Kralj, M.; Basarić, N., Competing Photochemical Reactions of Bisnaphthols and their Photoinduced Antiproliferative Activity, *Photochem. Photobiol. Sci*. **2019**, *18*, 1197-1211.